

The Dispersed Young Population in Orion

César Briceño

Centro de Investigaciones de Astronomía (CIDA)
Apartado Postal 264
Mérida 5101-A
Venezuela

Abstract. The Orion OB1 Association, at a distance of roughly 400 pc and spanning over 200 deg^2 on the sky, is one of the largest and nearest OB associations. With a wide range of ages and environmental conditions, Orion is an ideal laboratory for investigating fundamental questions related to the birth of stars and planetary systems. This rich region exhibits all stages of the star formation process, from very young, embedded clusters, to older, fully exposed young stars; it also harbors dense clusters and widely spread populations in vast, low stellar density areas. This review focuses on the later, namely, the low-mass ($M_* \lesssim 2M_\odot$), pre-main sequence population spread over wide spatial scales in Orion OB1, mostly in the off-cloud areas. As ongoing studies yield more complete censuses it becomes clearer that this "distributed" or non-clustered population, is as numerous as that located in the molecular clouds; modern studies of star formation in Orion would be incomplete if they did not include this widely spread population.

1. Introduction

It has been recognized for quite some time that OB associations are the prime sites for star formation in our Galaxy (see review by Briceño et al. 2007a). Recent evidence shows that stars in these regions form not only in dense clusters (e.g. Gómez & Lada 1998; Lada & Lada 2003), but also in more loose aggregates, spread in large numbers over wide areas spanning tens or even hundreds of square degrees on the sky (Briceño et al. 2005; Slesnick et al. 2006). Ongoing surveys suggest that this "distributed" or non-clustered population, could be as numerous as that in clusters (Briceño et al. 2005; Gutermuth et al. 2006; Briceño et al. 2007a). While the earliest stages of stellar evolution must be probed with infrared and radio techniques that can peer into the embedded, very young (ages $\lesssim 1 \text{ Myr}$) on-cloud populations, many fundamental questions including lifetimes of molecular clouds, cluster dispersal, protoplanetary disk evolution and triggered star formation, can only be addressed by surveys of the older, off-cloud populations with ages $\sim 3 - 10 \text{ Myr}$. Modern studies of star formation in nearby stellar nurseries are incomplete if they do not include this widely spread population.

The Orion OB1 Association (Blaauw 1964), located well below the Galactic plane ($-11^\circ \gtrsim b \gtrsim -20^\circ$), at a distance of roughly 400 pc (Genzel & Stutzki 1989; Briceño et al. 2005; Hernández et al. 2005), and spanning over 200 deg^2 on the sky, is one of the two largest and nearest OB associations (the other one being Scorpius-Centaurus, see the chapter by Preibisch & Mamajek). Blaauw (1964) quotes 56 massive stars with spectral types earlier than B2, more than Scorpius-Centaurus and Lacerta OB1, and only

slightly less than Cepheus. He estimates a total mass for Orion OB1 of $\sim 8 \times 10^3 M_{\odot}$, though this number is probably best interpreted as a lower limit, because it does not include the lower mass stars. With a wide range of ages and environmental conditions, Orion exhibits all stages of the star formation process, from very young, embedded clusters, to older, fully exposed OB associations, as well as both clustered and distributed populations. Therefore, this region is an ideal laboratory for investigating fundamental questions related to the birth of stars and planetary systems. Here we focus on the low-mass ($M_{*} \lesssim 2M_{\odot}$), pre-main sequence population widely distributed in the Orion OB1 association, in the general area within $\alpha_{J2000} \sim 5\text{h}$ to 6h and $\delta_{J2000} = \sim +6^{\circ}$ to -6° . Regions like λ Orionis, which is the subject of the chapter by Mathieu in this volume, are not discussed here, nor the population in the Orion molecular clouds (chapters by Peterson & Megeath, Allen & Hillenbrand), or clusters like the Orion Nebula Cluster (ONC), discussed by Muench et al., or σ Ori, which is discussed in the chapter by Walter et al.

2. The Orion OB1 Association: Historical Overview

Blaauw (1964, 1991) was the first to identify four major subgroups in Orion, mostly based on the distribution of O and B type stars, which he named 1a through 1d. Orion OB1 encompasses a giant molecular cloud system revealed in large scale ^{12}CO radio maps (e.g. Kutner et al. 1971; Maddalena et al. 1986). The two main structures are known as the A and B clouds (e.g. see in this volume Figure 8 in chapter by Bally et al., also chapters by Allen & Davies and Peterson & Megeath). The northernmost is the B cloud, showing extended ^{12}CO emission spanning roughly 8° , from the L1617 cloud (Lynds 1962) at $\delta \sim +5^{\circ}$ down to the Horsehead Nebula and NGC 2024.

Warren & Hesser (1977) carried out a detailed photometric study of Blaauw's sub-associations, and were the first to formally assign boundaries between them (Figure 1). The Ori OB1a sub-association, encompassing roughly $13^{\circ} \times 8^{\circ}$, a projected dimension of $\sim 74 \times 46$ pc, extends mostly north and west of the Orion Belt. Large scale radio (e.g. Maddalena et al. 1986) and visual extinction maps (Schlegel et al. 1998) show that this wide area is mostly devoid of gas. The Ori OB1b region extends over $\sim 4.6^{\circ} \times 2.5^{\circ}$, a projected dimension of 35×19 pc, encompassing the three belt stars δ , ϵ and ζ Ori, σ Ori with its associated young cluster, and part of the Orion B molecular cloud, in which are located the embedded clusters NGC 2023, 2024, NGC 2068 and 2071. The Ori OB1c group as defined by Blaauw (1964) includes the general region of the Orion Sword ($\sim 2 \text{ deg}^2$); however, Warren & Hesser (1977) outline a much larger area for 1c ($\sim 80 \text{ deg}^2$). The Ori OB1d group is limited to a small area of $\lesssim 0.5 \text{ deg}^2$, encompassing essentially the Trapezium or ONC. This general subdivision, based on the early type stellar population in Orion, was carried further by other studies. Warren & Hesser (1978) divided group 1b into three subgroups, mainly motivated by Hardie et al. (1964) and Crawford & Barnes (1966) who, based on UBV photometric parallaxes, found a gradient of distances for the three belt stars, with δ Ori being the nearest and ζ Ori the farthest. However, more recently Brown et al. (1994), using Walraven photometry of the early type stars in this region, found no significant differences in distances among the three belt stars, and no trend in the E-W direction. Here we will adopt the initial, broader subdivisions proposed by Blaauw. As we will discuss further on, the issue of subgrouping in Orion as a whole is probably more complicated than previously thought,

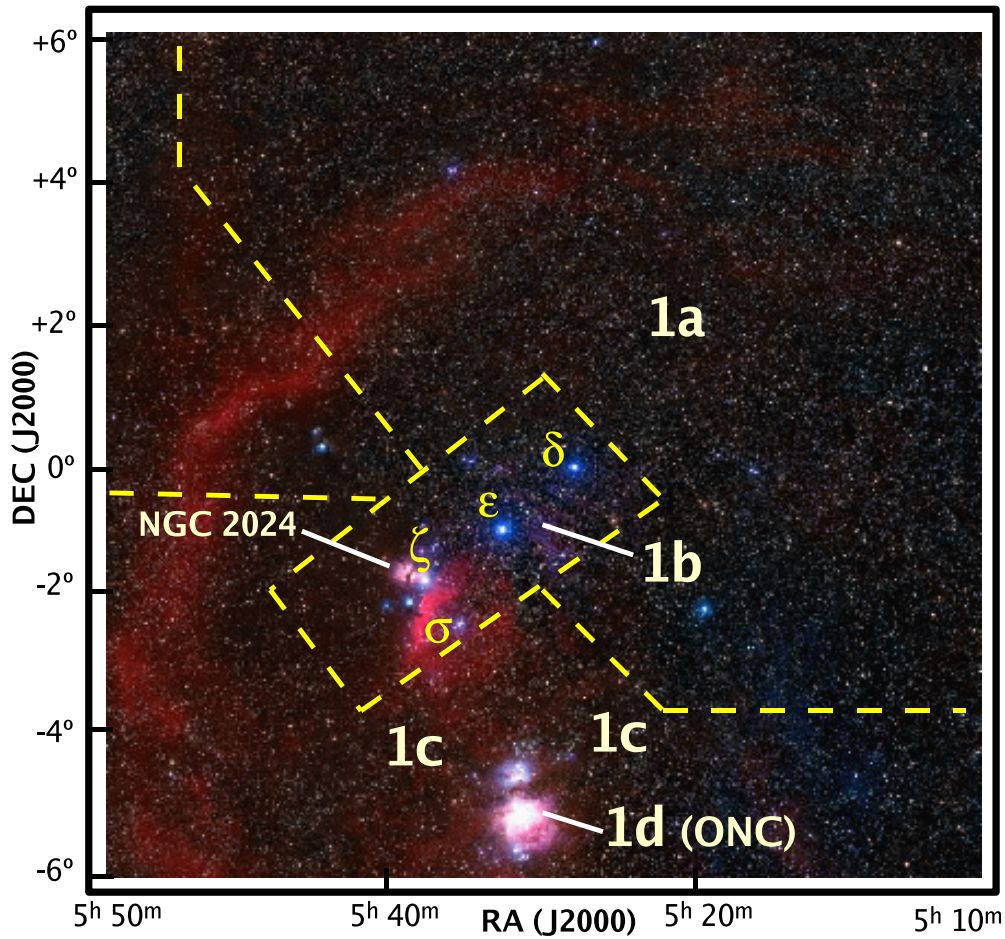


Figure 1. Optical wide field image of $\sim 150\text{deg}^2$ encompassing the Orion OB1 association. The three Orion belt stars are indicated, as well as the star σ Ori. The dashed lines outline the boundaries of each sub-association as described in Warren & Hesser (1977). The older, more extended Ori OB1a region spans the area roughly N-W of the Orion belt. The Ori OB1b sub-association corresponds to the area surrounding the three belt stars. The OB1c region roughly spans the Orion Sword area, around the Orion Nebula, while Ori OB1d corresponds essentially to the Orion Nebula Cluster.

and certainly a problem that cannot be properly investigated by studies of the early type stars alone.

The spatial distribution of the subgroups as depicted in Figure 4 of Blaauw (1964) shows an increasing degree of concentration going from 1a to 1c. If the subgroups are unbound and expanding, this suggests a sequence of decreasing ages. In fact, from the color-magnitude diagrams for the hottest stars in each subassociation, Blaauw provides ages of 12 Myr for 1a, 8 Myr for 1b, 6 Myr for 1c and ~ 4 Myr to 1d (though the kinematic age for the ONC is listed in his Table II as 0.3 Myr). Warren & Hesser (1977)

estimated ages of 7.9, 5.1, 3.7 and $\lesssim 0.5$ Myr for Ori OB1a through 1d, respectively. More recently, Brown et al. (1994) derived ages for the various subgroups in Orion OB1, using isochrone fitting in the $\log g$ - $\log T_{eff}$ plane. The resulting ages were 11.4 ± 1.9 , 1.7 ± 1.1 , and $4.6_{-2.1}^{+1.8}$ Myr for 1a, 1b and 1c respectively, and < 1 Myr for group 1d. The newer results derived from low-mass stars provide better constraints to the ages of each region, as is shown in Sect. 4.. The trend seen initially, of Ori OB1a being the oldest sub-association is confirmed, but the actual age of OB1b is closer to the initial estimates, and significantly older than the value derived by Brown et al. (1994).

The distance to Orion OB1 was quoted by Blaauw (1964) as 460 pc. Warren & Hesser (1977) determined distances of 400, 430, 430 and 480 for Ori OB1a, 1b, 1c and 1d respectively. Brown et al. (1994) used main sequence fitting for the OB stars in the subassociations to estimate distances and ages. They found a difference between 1a and 1b, with 1b having a similar distance as that of the molecular cloud, ~ 440 pc (Genzel et al. 1981), while 1a is closer, at ~ 330 pc. Stars in Brown et al. (1994) were observed by *Hipparcos*; these results were analyzed by Brown et al. (1999), who confirmed the distance difference between 1a and 1b, although there were substantial observational errors in the parallaxes of individual stars. Hernández et al. (2005) used *Hipparcos* parallaxes for a subset of stars in Ori OB1a and OB1b, and found distances of 335 ± 13 pc for OB1a and 443 ± 16 pc for OB1bc.

Table 1 summarizes our knowledge of the global properties of the Orion OB1 subgroups, based on studies of early type stars (spectral types O, B and A).

Table 1. Orion OB1 properties derived from high-mass stars

| Group | Age(Bw64) (Myr) | Age (WH77) (Myr) | Age (Bw91) (Myr) | Age (Br94) (Myr) | D (pc) | No. Stars ($M_* > 2M_\odot$) |
|-------|--------------------|---------------------|---------------------|---------------------|-----------|-----------------------------------|
| a | 12 | 7.9 | 12 | 11.4 ± 1.9 | 330 | 234 |
| b | 8 | 5.1 | 7 | 1.7 ± 1.1 | 440 | 123 |
| c | 6 | 3.7 | 3? | $4.6_{-2.1}^{+1.8}$ | 460 | 246 |
| d | 4 | $\lesssim 0.5$ | 0 | $\lesssim 1$ | 480 | 62 |

Note: ages are from Blaauw (1964); Warren & Hesser (1977); Blaauw (1991); Brown et al. (1994). Distances and the number of massive stars in each region are from Brown et al. (1994), except for 1d, for which the number of stars with $M_* > 2M_\odot$ was estimated from Table 3 of Hillenbrand (1997).

3. Wide Area Searches for Low-mass, Young Stars in Orion: Detection Techniques

Despite being one of the best studied star-forming regions in the solar vicinity, comprehensive studies of the widely spread, low-mass, pre-main sequence (PMS) population across Orion OB1 started to become available only quite recently. The reason has been that, unlike what happens with the very young on-cloud populations, it is much more difficult to find these older, more distributed low-mass stars, because the parent molecular clouds dissipate after a few Myr and no longer serve as markers of these populations (see also the discussion in Sect. 1 of the chapter by Preibisch and Mamajek). In order to find these widely spread stars unbiased, wide-field surveys spanning tens or even hundreds of square degrees are required; such sensitive searches have been difficult to carry

out in the past. The majority of studies so far have concentrated on small areas with high stellar density like the Orion Nebula (e.g. Baade & Minkowski 1937; Johnson 1965; Walker 1969; Herbig & Terndrup 1986; Hillenbrand 1997; Hillenbrand et al. 1998; Herbst et al. 2000; Rebull et al. 2000; Feigelson et al. 2003; Sicilia-Aguilar et al. 2005; Preibisch et al. 2005; Stassun et al. 2006), σ Orionis (e.g. Walter et al. 1997; Béjar et al. 1999; Zapatero Osorio et al. 2002; Barrado y Navascués et al. 2003; Sherry et al. 2004; Kenyon et al. 2005; Jeffries et al. 2006), NGC 2024 (e.g. Freyberg & Schmitt 1995; Comerón et al. 1996; Haisch et al. 2000, 2001; Skinner et al. 2003; Levine et al. 2006), NGC 2068 (e.g. Herbig & Kuhl 1963; Muzerolle et al. 2005), and NGC 2071 (e.g. Harvey et al. 1979; Dahari & Lada 1999; Muzerolle et al. 2005) clusters. Before considering the various search techniques used to find low-mass PMS stars in the wide off-cloud areas in OB associations like Orion OB1, it is useful to briefly review the observational properties of these young low-mass objects.

Low-mass PMS stars, known collectively as T Tauri stars (TTS), were originally characterized by their late spectral types (G-M), strong emission lines (especially $H\alpha$), and significant variability in brightness at most wavelengths; many are also found spatially associated with regions of dark nebulosity (Joy 1945). Stars resembling the original variables first identified as TTS are currently called "strong emission" or Classical TTS (CTTS). Subsequent spectroscopic studies of the Ca II H and K lines and the first X-ray observations with the *Einstein* X-ray observatory (Feigelson & DeCampi 1981; Walter & Kuhl 1981) revealed surprisingly strong X-ray activity in TTS, exceeding the solar levels by several orders of magnitude, and also revealed a population of X-ray strong objects lacking the optical signposts of CTTS, like strong $H\alpha$ emission. These stars, initially called "naked-T Tauri stars" (Walter & Myers 1986), are now widely known as "weak-line" TTS (WTTS) after Herbig & Bell (1988). At first, the CTTS/WTTS dividing line was set at $W(H\alpha) = 10 \text{ \AA}$. Recently, White & Basri (2003); Barrado y Navascués & Martín (2003) revisited the WTTS/CTTS classification and suggested a modified criterion that takes into account the contrast effect in $H\alpha$ emission as a function of spectral type in stars cooler than late K.

3.1. Objective Prism Searches

The strong $H\alpha$ emission characteristic of CTTS made large area searches using photographic plates and objective prisms on wide field instruments like Schmidt telescopes (e.g. Sanduleak 1971, in Orion) particularly appealing. These very low resolution spectroscopic surveys (typical dispersions of $\sim 1700 \text{ \AA/mm}$ at $H\alpha$) provided large area coverage, allowed estimates of spectral types and a qualitative assessment of the strength of prominent emission lines. In the Orion OB1 association, the most systematic search was that done with the 1m Kiso Schmidt (Kogure et al. 1989; Wiramihardja et al. 1989; Wiramihardja et al. 1991; Wiramihardja et al. 1993) covering roughly 150 square degrees and detecting ~ 1200 emission line stars, many of which were argued to be likely TTS (Figure 2). Weaver & Babcock (2004) recently identified 63 $H\alpha$ emitting objects in a deep objective prism survey of the σ Orionis region.

The main limitation of this technique is the strong bias towards $H\alpha$ -strong PMS stars; few WTTS can be detected at the resolution of objective prisms (c.f. Briceño et al. 1999). In fact, out of 25 Kiso sources matching confirmed PMS stars in Briceño et al. (2005), only 3 objects (12%) are WTTS; therefore, specially in somewhat older regions, in which most TTS are of the WTTS type, objective prism searches miss nearly 90% of the PMS stars. Another caveat is contamination by field stars. The spatial distribution

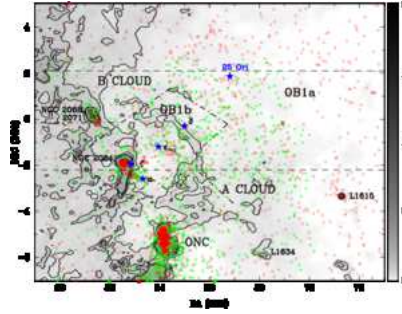


Figure 2. Spatial distribution of $H\alpha$ emission and X-ray sources in Orion listed in the SIMBAD database. Small red circles are X-ray sources from pointed observations in the Orion clusters (e.g., ONC, NGC2024, NGC 2068/2071 Feigelson et al. 2002; Gagné & Caillault 1994; Getman et al. 2005; Ramírez et al. 2004; Rebull et al. 2000; Tsujimoto et al. 2002; Yamauchi et al. 1996), and ROSAT All-Sky Survey sources over the entire OB association (Sterzik et al. 1995; Voges et al. 1999). Green starred symbols indicate Kiso $H\alpha$ emission line objects (Kogure et al. 1989; Wiramihardja et al. 1989; Wiramihardja et al. 1991; Wiramihardja et al. 1993). The greyscale map shows the integrated ^{13}CO emissivity from Bally et al. (1987) covering the range from 0.5 to 20 K km s^{-1} . Isocontours correspond to the extinction map of Schlegel et al. (1998). Dot-dash lines show the Warren & Hesser (1977) boundaries for Ori OB1a and OB1b. The Orion belt stars, σ Ori and 25 Ori are indicated by large blue starred symbols; also labeled are the the outlying clouds L1615 and L1634.

of the Kiso sources has been useful to outline the youngest regions in Orion (Figure 2) where the highest concentrations of CTTS are located (Gómez & Lada 1998), but these samples can be dominated by objects like dMe stars in regions far from the molecular clouds, in which the CTTS/WTTS fraction is small. Briceño et al. (2005) find a CTTS/WTTS fraction of 11% in Ori OB1a, and a slightly higher value of 23% in Ori OB1b, indicating that the Kiso searches missed the majority of the young population in these regions. Only about 50% of the 218 Kiso $H\alpha$ sources located within the 68 deg^2 area surveyed by Briceño et al. (2005) in the OB1a and OB1b sub-associations, fall above the Zero Age Main Sequence (ZAMS) in the V vs. $V - I_C$ color-magnitude diagram, and just 33% of those are found to be variable (a sign that they may be true TTS, see Sect. 3.4.), as would be expected for TTS (Figure 3); these numbers suggest that the overall fraction of PMS objects among Kiso objects is probably not much greater than $\sim 30\%$, and likely less in the extended area off the main Orion clouds. Therefore, objective prism studies require follow up spectroscopy to confirm membership.

3.2. X-ray Surveys

X-ray observations are a well established tool to find active stars, like young PMS stars. For nearby OB associations, which typically cover areas in the sky much larger than the field of view of X-ray observatories, deep pointed observations spanning many square degrees are usually not feasible. However, large scale shallow surveys have been conducted with great success. The ROSAT All Sky Survey provided coverage of the whole sky in the 0.1 – 2.4 keV soft X-ray band. With a mean limiting flux of about $2 \times 10^{-13} \text{ erg s}^{-1} \text{ cm}^2$, this survey provided a spatially complete, flux-limited sample of X-ray sources that led to the detection of hundreds of candidate PMS stars

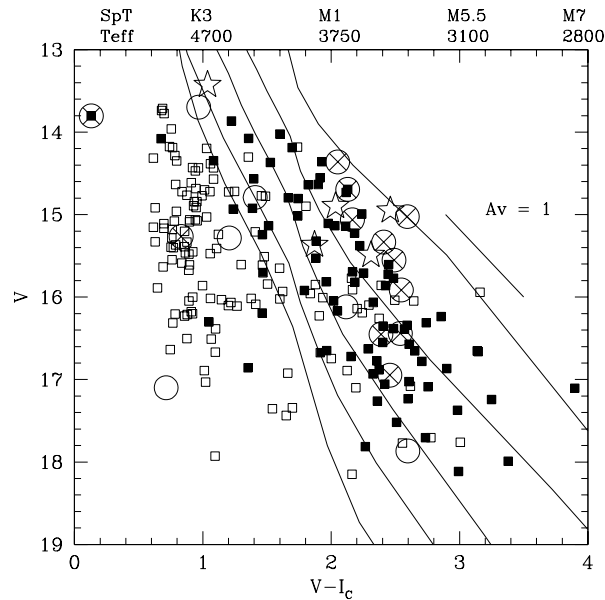


Figure 3. Color-magnitude diagram for a subset of $H\alpha$ -emitting stars from the Kiso-Schmidt survey, and X-ray sources, in the Orion star forming region. Kiso stars detected as variables by Briceño et al. (2005) are indicated by solid squares; non-variable objects are plotted as open squares. X-ray sources are plotted as circles, and those detected as variables by Briceño et al. (2005) are highlighted by a \times symbol. The five large stars correspond to previously known TTS in the area, listed in the Herbig & Bell (1988) catalog. Solid lines are isochrones from Siess et al. (2000) at 1, 3, 10, 30, 100 Myr.

across all of Orion (Sterzik et al. 1995). Figure 2 shows the spatial distribution of all X-ray sources, both in deep, pointed observations in selected regions like the ONC, and NGC 2024, 2068, 2071 (Feigelson et al. 2002; Gagné & Caillault 1994; Getman et al. 2005; Ramírez et al. 2004; Rebull et al. 2000; Tsujimoto et al. 2002; Yamauchi et al. 1996) and the ROSAT All-Sky Survey sources spread over the entire OB association (Sterzik et al. 1995; Voges et al. 1999). The majority of the X-ray sources are concentrated toward the best known clusters inside the Orion A and B clouds: the ONC, NGC 2024, 2068 and 2071; this is not surprising, since most deep pointings with X-ray observatories like *Einstein*, *ROSAT*, and more recently *ASCA*, *Chandra* and *XMM* have been done in these regions. The ROSAT All-Sky Survey sources in the off-cloud areas spanning Ori OB1a and OB1b are distributed much more uniformly, except for the strong concentration near the early type star 25 Ori and another overdensity in the L1615 cloud. The PMS population in L1615 is discussed in the chapter by Alcalá et al. in this book. Sterzik et al. (1995) found a density enhancement of ROSAT All-Sky Survey sources with a roughly circular extent of $\sim 5^\circ$, centered at $\alpha \approx 82^\circ$, $\delta \approx +3^\circ$. Briceño et al. (2005) identified a grouping of PMS stars around 25 Ori, located at $\alpha_{J2000} \sim 80.8^\circ$ and $\delta_{J2000} \sim +1.8^\circ$ which is characterized as a populous young cluster by Briceño et al. (2007a, see Sect. 4.3. below).

The ROSAT All-Sky Survey flux limit corresponds to X-ray luminosities of about $10^{30} \text{ erg s}^{-1}$ at the distance of Orion OB1 ($\sim 400 \text{ pc}$). This is equivalent to $V \sim 15$ (assuming a typical $\log L_X/L_{bol} = -3.6$, Wolk et al. 2005), the magnitude of a few

Myr old K7 star ($M_* \sim 0.8M_\odot$; Baraffe et al. 1998; Siess et al. 2000). This implies that the ROSAT All-Sky Survey data are essentially complete only for $M \geq 1 M_\odot$ PMS stars in those regions. Also, Briceño et al. (1997) showed that, because X-ray activity decays slowly during the first 100 Myr in solar-like stars, the ROSAT All-Sky Survey candidate PMS samples in areas far from molecular clouds suffered from significant contamination by young main sequence stars of ages up to $\sim 10^8$ yr. These limitations have to be kept in mind when working with X-ray selected samples; at any rate, follow-up observations are necessary to determine the nature of the objects.

3.3. Single-epoch Optical Photometry

Single epoch optical photometric surveys are frequently used to select candidate low-mass members of young clusters or associations. Candidates are usually selected by their location in the optical color-magnitude diagram (CMD) above the ZAMS. The locus in which low-mass PMS stars are located is usually defined by either a known (spectroscopically confirmed) population of PMS stars, by comparison with theoretical model isochrones, or because the PMS population of the association is clearly visible as a concentration on the CMD (e.g., Figure 5). The main advantage of photometric selection is that for a specified amount of time on any given telescope a region of the sky can be surveyed to a fainter limit than can be done by a variability survey, and low-mass candidate members can be selected without regard to their brightness variations, which could bias selection against objects with small amplitudes in their light curves. The disadvantage of this technique is that there is inevitably some contamination by foreground field stars and background giants; in large areas with a lower density of low-mass association members, such as Orion OB1b or Orion OB1a the field star contamination can be large enough to make it difficult to see the PMS locus (see below).

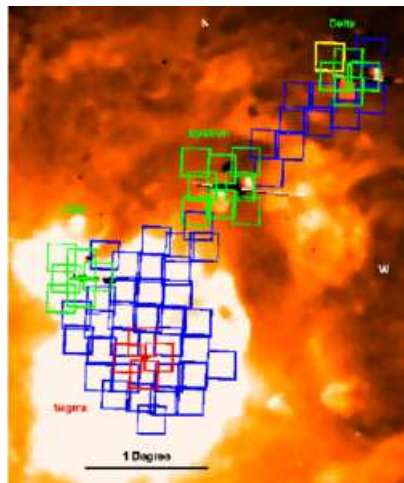


Figure 4. Fields observed by W. Sherry in Ori OB1b. Colors indicate different observing runs. The background image is from the Southern $H\alpha$ All Sky Survey (Gaustad et al. 2001). The bright regions are the $H\alpha$ emission near σ Ori and ζ Ori. The three belt stars are the dark marks running from left to upper right.

The only moderately wide angle, single epoch photometric survey in the Orion OB1 association has been carried out by Sherry (2003), who studied a ~ 5 deg² area

in Ori OB1b and a small part of Ori OB1a, mostly around the belt stars (Figure 4). A subset of this study, centered on σ Ori, was reported by Sherry et al. (2004). Most of the fields shown in Figure 4 were observed in the BVRI filters with the 0.9m telescope at CTIO, reaching limiting magnitudes $V \sim 21$ and $I_C \sim 19 - 20$. The identification of the PMS population was done using a statistical approach, fitting the PMS locus in color-magnitude diagrams, no spectroscopic confirmation was done. In Table 3.4 of his PhD thesis, Sherry provides the number of candidate PMS stars in each region of his survey, totaling ~ 800 objects in the mass range $M \sim 0.15 - 1 M_{\odot}$. The stars are spread over a small portion of the Ori OB1a and OB1b regions, and the immediate surroundings of σ Ori and ζ Ori. Data for individual stars only exist for the likely PMS members of the σ Ori cluster (see Table 4 of Sherry et al. 2004).

3.4. Variability Surveys

Optical photometric variability is one of the defining characteristics of PMS stars (Joy 1945; Herbig 1962). However, due to limitations in the size of CCD detectors, past work on photometric variability of young stars have concentrated on follow up studies of selected samples, that had been identified as PMS objects by some other means. Only very recently has the potential of variability as a technique to pick out young stars amongst the field population started to be realized (Briceño et al. 2001; Lamm et al. 2004).

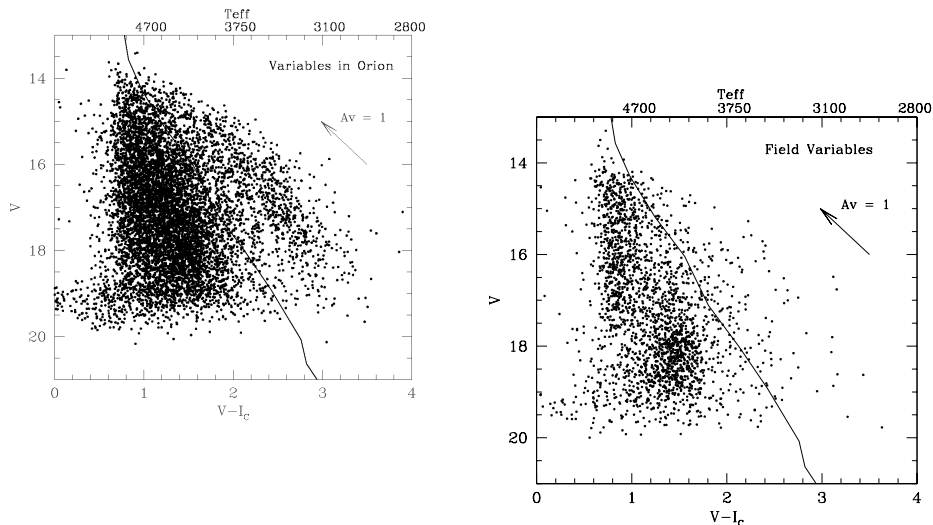


Figure 5. Color-magnitude diagrams for stars selected as variable in Briceño et al. (2005). Left panel: all variables detected in a 2.3° wide strip centered at $\delta = -1^{\circ}$ and from $\alpha = 5^{\text{h}}$ to 6^{h} , going over part of Ori OB1a and Ori OB1b. Right panel: control field off Orion; stars in the same strip, with $\alpha = 4^{\text{h}}48^{\text{m}} - 5^{\text{h}}00^{\text{m}}$. In both panels the solid line represents the ZAMS at the distance to Orion ($d \sim 400$ pc; Briceño et al. 2005). The PMS locus is densely populated in the CMD of the Orion OB1 region.

Briceño et al. (2001) showed that in surveys spanning wide solid angles, the large number of objects limits the usefulness of traditional, single epoch CMDs to single out the PMS locus. They show in their Figure 2 that even in a modest region of $\sim 10 \text{ deg}^2$ towards Ori OB1b there can be of the order of 4000 objects above the ZAMS down to $V \sim 19.5$; but once object lists are filtered by their variability, only $\lesssim 10\%$ remain above the ZAMS. Moreover, selection of variable stars above the ZAMS clearly picks a significant fraction of the young members of Orion, as can be seen in Figure 5 (from Briceño et al. 2005), which presents a comparison between CMDs for a region in OB1b ($\alpha_{J2000} \sim 82.4^\circ, \delta_{J2000} \sim 0.3^\circ$) and a control field ($\alpha_{J2000} \sim 67.5^\circ, \delta_{J2000} \sim 0^\circ$), located well off Orion; the Orion field exhibits an excess of objects above the ZAMS not present in the control field, even after taking into account that the Orion region has a higher density of stars because it is closer to the Galactic plane. In the Orion field the fraction of variables above the ZAMS is 19% compared to 10% in the control field, a factor of ~ 2 overdensity. However, the densest concentration of points in the color-magnitude diagram for the Orion field occurs at roughly 1 magnitude above the ZAMS. Comparing this locus in both panels of Figure 5, results in the Orion field having a factor of $3\times$ more objects than the control field.

Recently, four major studies have used large format CCD cameras installed on wide-field telescopes to conduct multi-epoch, photometric surveys that use variability to pick out candidate TTS over extended areas in Orion. Briceño et al. (2001, 2005, 2007b) have done a VRI variability survey using the QUEST I CCD Mosaic Camera (Baltay et al. 2002) installed on the Venezuela 1m Schmidt telescope, over an area of $\gtrsim 150$ square degrees in the Orion OB1 association (CIDA Variability Survey of Orion - CVSO). The limiting magnitudes are $V \sim 19.7$ and $I_C \sim 19$. They used a χ^2 test on the normalized V -band magnitudes to select variable stars; if the probability that the dispersion is due to random errors was very low (≤ 0.01), the object was flagged as variable. The minimum Δmag they detected is 0.06 for $V = 15$, 0.09 for $V = 17$ and 0.30 for $V = 19$. Figure 6 shows the distribution of V -band amplitudes for CTTS and WTTS from Briceño et al. (2005). While both type of stars have a ΔV peaking at 0.2 mag the CTTS have a larger spread in amplitudes up to a few magnitudes.

McGehee et al. (2005) analyzed 9 repeated observations over 25 deg^2 in Orion, obtained with the Sloan Digital Sky Survey (SDSS). They selected 507 stars that met their variability criterion in the SDSS g -band. They did not obtain follow up spectra of their candidates, rather, they made a statistical analysis to search for photometric accretion-related signatures. McGehee (2006) studied a 2.5° wide strip from $\alpha_{J2000} = 5\text{h}$ to 6h , encompassing 37 deg^2 within the area of the CVSO survey. He applied reddening invariant indices to select candidate TTS. Furthermore, McGehee (2006) use the fact that CTTS are more highly variable than WTTS (Figure 6), as one of the criteria to distinguish one type of TTS from the other solely on the basis of the photometric data. McGehee (2006) used the cumulative distribution function to set a threshold value of σ_V to identify TTS candidates and distinguish WTTS from CTTS. In general, he identified TTS candidates as those objects with $\sigma_V \geq 0.05 \text{ mag}$ (in addition to fulfilling other criteria such as appropriate optical and near-IR colors), and CTTS as objects above a threshold $\sigma = 0.2 \text{ mag}$.

Restricted to a much smaller area, Scholz & Eislöffel (2005) carried out a multi-epoch study in the vicinity of ϵ Ori to explore the rotation and activity of very low-mass PMS objects. Lacking spectra, they selected 143 objects as young very low-mass stars and brown dwarfs, based on their variability and RIJK photometry being consistent

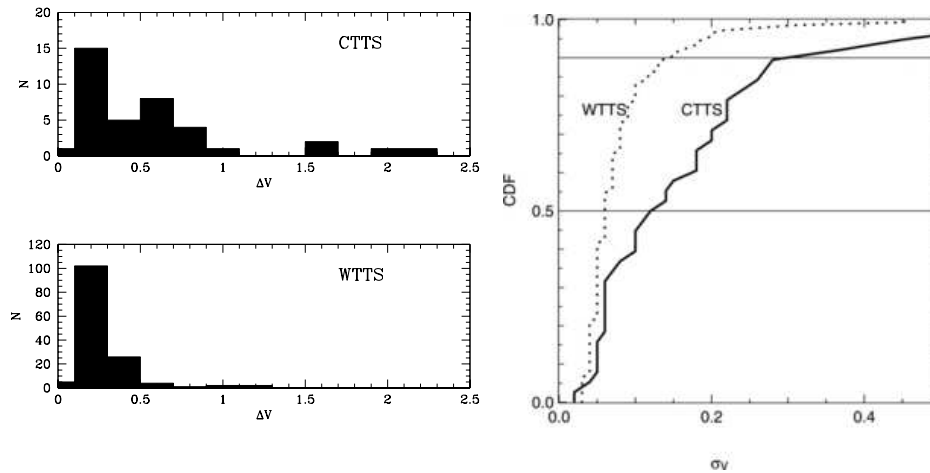


Figure 6. Left: Histograms showing the distribution of Δmag for Classical T Tauri stars (upper panel) and Weak-lined T Tauri stars (lower panel) in the CVSO (from Fig. 4 of Briceño et al. 2005). Right: Cumulative distribution functions (CDFs) of σ_V for spectroscopically confirmed WTTSs (dotted line) and CTTSs (solid line) in the sample of Briceño et al. (2005). As can also be seen in the left panel, it is clear that the CTTSs are much more highly variable than the WTTSs. The median value of σ_V , at CDF = 0.5, for the WTTSs and CTTSs is 0.06 and 0.12 mag, respectively. The 90th percentile values of σ_V for the WTTSs and CTTSs have a greater spread of 0.14 mag (from Fig.6 of McGehee 2006).

with membership in this young region. The variability of these objects was investigated using a densely sampled I-band time series covering four consecutive nights with a total of 129 data points per object.

The main disadvantages of variability surveys are that they are observationally intensive, not easy to carry out in highly oversubscribed telescopes, and that, as photometric errors increase toward fainter magnitudes, the incompleteness is also larger for lower masses, as more faint objects with small amplitude variations fail to be detected. However, quantitative estimates of the actual incompleteness are not yet available. As with other techniques, spectroscopic confirmation is important.

Spatial Distribution of Variable Candidate PMS Stars The CVSO has revealed a numerous PMS population in the age range $\sim 4 - 10$ Myr, largely discretized in distinct groups of stars (Briceño et al. 2005, 2007b). That stars are born in clusters and groups is known from studies of molecular clouds (Lada & Lada 2003), but that these groups remain as separate entities after the gas is removed is a new fact, attesting to the rapidness of molecular cloud dissipation.

Figure 7 shows the surface density of 2MASS sources, located above the ZAMS and flagged as variable, in the Ori OB 1a and 1b subassociations (data from Briceño et al. 2005, 2007b). The conspicuous overdensity at $\alpha_{J2000} = 81.2^\circ$, $\delta_{J2000} = +1.85^\circ$ marks the newly discovered 25 Ori cluster (“25 Ori”; see Sect. 4.3. Briceño et al. 2007b). Other overdensities or “clumps” are also evident in Figure 7; one corresponds to the well known σ Ori cluster, with a peak stellar density similar to that of 25 Ori.

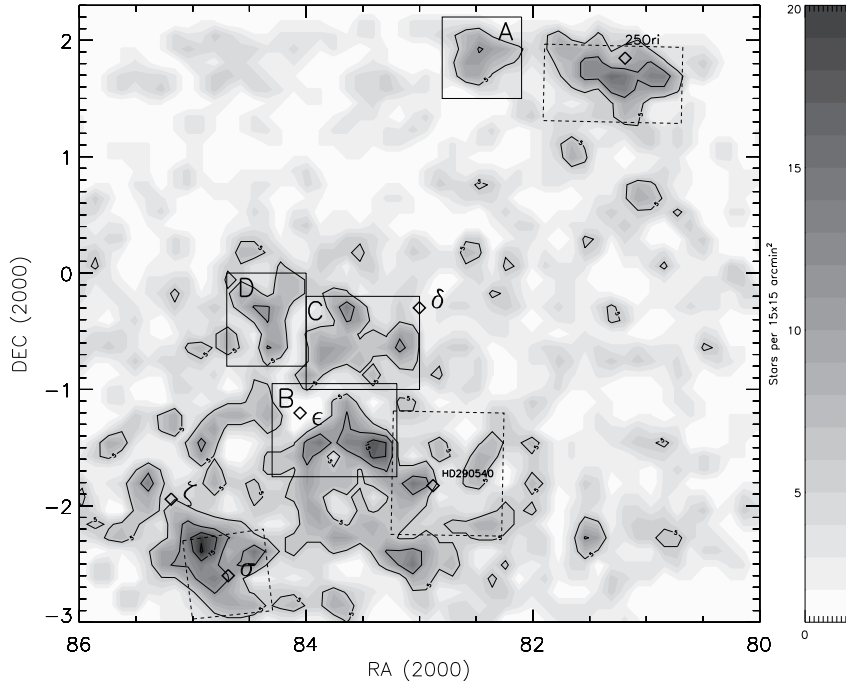


Figure 7. Surface density of 2MASS sources, located above the ZAMS and flagged as variable, in Ori OB1a and OB1b (Briceño et al. 2008). In the upper right is the 25 Ori cluster (Briceño et al. 2007b); in the lower left the σ Ori cluster (Hernández et al. 2007a). Dashed-line rectangles indicate the regions studied by Hernández et al. (2007b); additional fields (solid rectangles) are being observed with Spitzer by Briceño and collaborators as of the writing of this chapter. The three stars of the Orion belt are labeled.

McGehee (2006) constructed a similar surface density map to investigate the distribution of candidate TTS picked out on the basis of $\sigma_g > 0.05$ (see his Figure 8). He recognized overdensities corresponding to the southern tip of the 25 Ori group, the Orion OB1b subassociation, and the NGC 2068/NGC 2071 star formation site in the Lynds 1630 cloud. The over density that McGehee (2006) finds at the south tip of 25 Ori corresponds to the two small clumps at $\alpha_{J2000} = 81.0^\circ, \delta_{J2000} = +0.7^\circ$ and $\alpha_{J2000} = 81.6^\circ, \delta_{J2000} = +1.0^\circ$ in the map of Figure 7, while the overdensity he sees in Ori OB1b, located at $\alpha_{J2000} = 83.5^\circ, \delta_{J2000} = -0.5^\circ$, corresponds to field C in Figure 7.

These surface density maps demonstrate that variability selection can trace quite well the young population in these off-cloud regions.

3.5. Combination of Single-epoch Optical and Near-IR Photometry

Single-epoch photometry combining optical and near-IR passbands has been successfully applied to wide area searches for very low-mass PMS objects and young brown dwarfs (e.g. Briceño et al. 2002; Luhman et al. 2003b). In Orion OB1, Béjar et al. (2003) used I, Z and J-band photometry to search for very low-mass PMS stars and young brown dwarfs in the vicinity of the Orion belt star ϵ Ori, spanning an area

of 1000 arcmin² and reaching a limiting magnitude $I = 22$. From the I, I-Z color-magnitude diagram they selected 123 red candidates.

More recently, Downes et al. (2008) coadded the existing many epochs of the CVSO (Briceño et al. 2005) to produce single deep R and I-band images, with 3σ limiting magnitudes of $R_{lim} = 21.5$ and $I_{lim} = 20.7$, and completeness limits of $R_{com} = 20.3$ and $I_{com} = 19.0$, spanning an area of ~ 22 deg² in the Ori OB1a and OB1b subassociations. The deep optical imaging, combined with 2MASS JHK data yield optical/near-IR color-magnitude and color-color diagrams, that have enabled them to conduct the first sensitive survey for the lowest mass PMS stars and young brown dwarfs within the large area observed by the CVSO.

3.6. Archival Searches: Virtual Observatory

In a recent work, Caballero & Solano (2008) used Virtual Observatory¹ tools like Aladin² and TOPCAT³ to search and combine data from the Tycho-2, DENIS and 2MASS catalogues, together with photometric, spectroscopic X-ray and astrometric data from the literature to look for candidate members of the Ori OB1b subassociation in two 45 arcmin radius fields centered on the belt stars δ Ori and ϵ Ori. For the bright, early type stars (mostly B and A spectral types) they used optical-near infrared color-magnitude diagrams, the Tycho-2 proper motions, IRAS fluxes and spectroscopic data from the literature to identify likely members. To look for lower mass stars they cross-correlated the DENIS and 2MASS catalogues, and used indicators of youth, like H α or X-ray emission, and for those cases for which spectra are available, Li I in absorption or weak Na I lines indicative of low gravity. In all, they identified 78 bright, early-type stars, and 58 intermediate to low-mass stars, all showing signatures of youth; they also produced a list of 373 photometric candidates.

4. The Dispersed PMS Population in Orion OB1a and OB1b

4.1. Low-mass PMS Stars

Low-resolution follow up spectra are necessary to provide confirmation of PMS low-mass stars. These objects can be reliably identified through optical spectroscopy by the presence of: (1) H α emission, strong in CTTS, which exhibit equivalent widths $W(\text{H}\alpha) \geq 10$ Å at M0, with larger values at later spectral types (See White & Basri 2003; Barrado y Navascués & Martín 2003), and weak (a few Å) in non-accreting stars, or WTTS; (2) the Li I $\lambda 6707$ Å line strongly in absorption in late type stars (\sim K2 and later; e.g. Briceño et al. 1997)⁴; (3) a weak Na I doublet at 8183 and 8195 Å, an indicator of surface gravity.

¹<http://www.ivoa.net>

²<http://aladin.u-strasbg.fr/aladin.gml>

³<http://www.star.bris.ac.uk/mbt/topcat/>

⁴It is difficult to use the Li I line to select PMS stars of G and early K spectral types, because in these objects of somewhat higher masses, lithium suffers little depletion during the PMS phase; therefore, they can arrive at the ZAMS with Li I values similar to the expected primordial abundance. The reason is that in these stars the convection zone is much shallower, such that material from the photosphere is not efficiently mixed at depths where the temperature is high enough to burn Li.

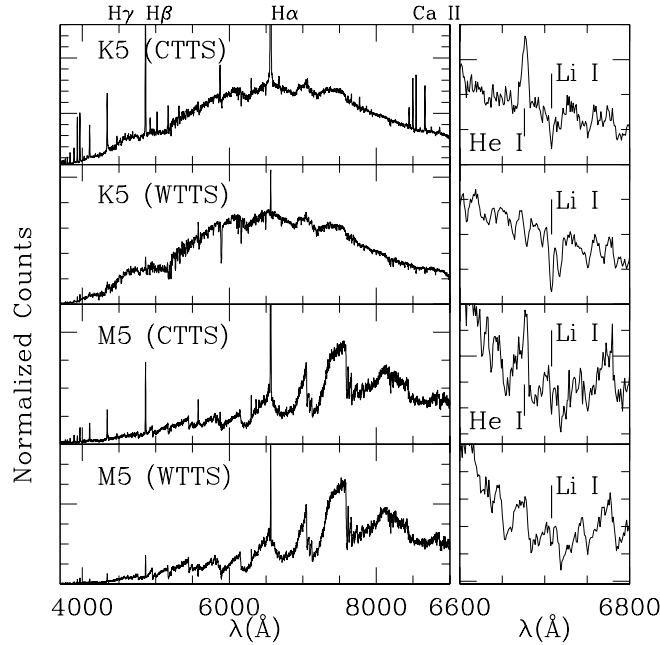


Figure 8. Spectra of members of the Orion OB1 association, obtained with the multi-fiber spectrograph Hectospec at the 6.5m MMT (Briceño et al. 2008). The upper panels show two K5-type PMS objects, an accreting CTTS and a non-accreting WTTS. For comparison the lower panels show two late spectral type members (M5). On the right are the wavelength regions around Li I $\lambda 6707$ Å line for each star. The Li I line is seen clearly in absorption in all objects, next to the Ca I line at 6715 Å. In the CTTS the He I line at 6676 Å is also seen in emission.

Figure 8 shows typical low-resolution (~ 6 Å) spectra of Orion PMS members, from K5 to M5 objects, and both CTTS and WTTS. The M5-type stars exhibit strong TiO bands at $\lambda \sim 5900, 6200, 6750, 7200, 7700$ Å, a feature of cool ($T_{\text{eff}} \sim 3200$ K; e.g. Kenyon & Hartmann 1995), very low mass ($M \sim 0.15 M_{\odot}$; Baraffe et al. 1998) PMS stars. Both CTTS show prominent Balmer lines characteristic of accreting young stars, and in the case of the K5-type CTTS also the Ca II IR triplet ($\lambda = 8498, 8542, 8662$ Å) is seen strongly in emission. The small panels show a zoom of the region around the Li I line, which is seen well in absorption in all four objects. Contaminating disk field dwarfs appear similar in all aspects to a WTTS, except in that they lack the Li I absorption line.

Figure 9 shows the Na I absorption lines ($\lambda 8183, 8195$) in several very low-mass and brown dwarf members of Orion OB1 (Downes et al. 2008), compared with field dwarfs, and with young very low-mass stars and brown dwarfs from the ~ 2 Myr old Chamaeleon I region. The weak Na I lines seen in the PMS Orion members are similar to those of the young Chamaeleon members, thus providing a strong criterion to select low-gravity young objects, still contracting toward the ZAMS, and clearly separating them from late spectral type, foreground dwarfs, which have much stronger lines.

Here we will consider as low-mass members of the Orion OB1 population only those stars which have been spectroscopically confirmed as late spectral type, PMS stars.

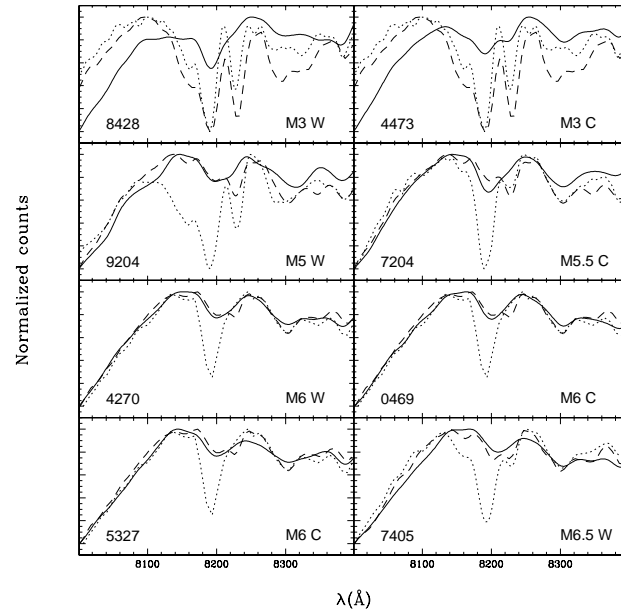


Figure 9. Na I $\lambda 8183, 8195$ absorption lines in very low-mass and brown dwarf members of Orion OB1 (solid line), compared with field dwarfs (dotted line; Kirkpatrick et al. 1999), and with young very low-mass stars and brown dwarfs from the Chamaeleon I region (~ 2 Myr old, dashed line; Luhman 2004a). New members and comparison templates have the same spectral types. Labels indicate spectral type and class (C=CTTS, W=WTTS). Adapted from Downes et al. (2008).

There are only a handful of major studies that have undertaken spectroscopic membership confirmation of low-mass PMS candidates, across the extended Orion OB1a and OB1b sub-associations. Figure 10 shows the spatial distribution of PMS stars from these various works across the Orion OB1 subassociation (Herbig & Bell 1988; Alcalá et al. 1996; Briceño et al. 2005, 2007b). To provide a complete view of objects known so far, we include in this figure the PMS objects identified in the L1615, L1616 and L1634 clouds; however, we do not discuss these regions further as they are the subject of the chapter by Alcalá et al. in this volume. Also, though a few objects are shown in the Orion B cloud, in and around NGC 2024, 2068 and 2071 (all in the dark cloud L1630), we will not focus here on these PMS populations since they are considered in the chapter by Gibb. Objects in the general ONC area are included in detail in the chapters by Peterson & Megeath, and by Muench et al.

Among the first TTS to be confirmed outside the ONC, are those from the *Second catalog of emission-line stars of the Orion population* (Herbig & Rao 1972), mostly from the Lick Observatory $H\alpha$ survey (identified with the acronym LkH α), which later were incorporated into the Herbig & Bell Catalog (HBC objects; Herbig & Bell 1988). Downes & Keyes (1988) and Maheswar et al. (2003) obtained optical spectroscopy of a number of $H\alpha$ emitting stars, brighter than $V \sim 13$, identified by Stephenson (1986) through objective prism spectroscopy over most of the sky above $b = 10^\circ$.

Alcalá et al. (1996) obtained follow-up spectroscopy, and photometry, of a sample of 181 candidate PMS stars from among 820 ROSAT All-Sky Survey sources detected over 450 deg^2 in Orion (see their Figure 4). They identified 112 TTS with spectral

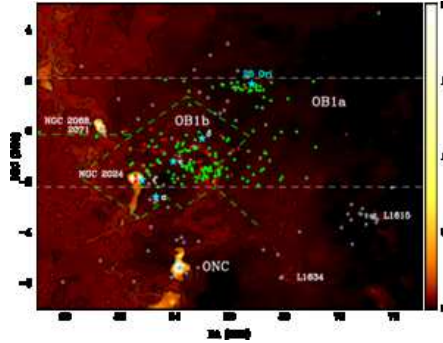


Figure 10. Large scale spatial distribution of spectroscopically confirmed, low-mass PMS stars in the Orion OB1a and OB1b sub-associations, projected on the dust emission map of Schlegel et al. (1998), represented in false color calibrated to $E(B - V)$ reddening in magnitudes. Contours are for $A_V = 0.5$ mag. Stars from Briceño et al. (2005) are indicated by green dots (WTTS), and red dots (CTTS). Small grey stars indicate PMS stars in the Herbig & Bell (1988) catalog. For clarity, the additional members of 25 Ori and a field in OB1b from Briceño et al. (2007b) are not plotted here. The horizontal dashed lines indicate the limits of the Briceño et al. (2005) survey. The dot-dashed lines show the boundaries of Ori OB1a and OB1b from Warren & Hesser (1977). The three belt stars and 25 Ori are plotted as large cyan starred symbols. Stars in the L1615 and L1634 clouds are not discussed here (see chapter by Alcalá et al.).

types later than F0, the majority of them WTTS; 54 of these objects are located in the 180 deg^2 area considered here, between $\alpha = 5\text{h}$ to 6h , and $\delta = -6^\circ$ to $+6^\circ$. However, this sample is probably contaminated by X-ray active, field stars, especially among the earlier spectral types, for which detection of Li I alone does not necessarily discriminate PMS objects from young stars on the ZAMS. In fact, the Alcalá et al. (1996) sample is composed mostly of G and early-K stars: 28% late F and G stars, 70% K stars (K0-K4=60%, K5-K7=10%) and 2% M stars. Briceño et al. (1997) predict that $\sim 40\%$ of the ROSAT All-Sky Survey sources in this region will be X-ray active, ZAMS stars with G spectral types, and the remaining $\sim 55\%$ will be field K stars, with most in the range K0-K4. All the G stars and most of the K stars in the Alcalá et al. (1996) sample have $H\alpha$ in absorption, consistent with a significant fraction of them being young main sequence stars. There is an excess of late K stars compared to the expected number of ZAMS stars, which is interpreted as being due to true PMS stars at these spectral types. In fact, the ROSAT All-Sky Survey sources are not uniformly distributed, but rather are seen mostly projected on or near the molecular clouds (See Figure 4 of Alcalá et al. 1996). The visual and near infrared magnitudes of many of the late K and M stars indicate that they are true TTS with ages of the order of a few times 10^6 yr .

In their large scale variability survey Briceño et al. (2001, 2005) confirmed 197 TTS through low-resolution ($\sim 6 \text{ \AA}$) spectroscopy, with spectral types from mid-K through $\sim M4$. Comparing with several evolutionary models they derived ages of 4-6 Myr for the Ori OB1b population and of 7-10 Myr for Ori OB1a. The majority of these stars are widely distributed over the 68 deg^2 studied in their initial release. However, on closer examination, a clear pattern can be seen in the distribution of CTTS and WTTS (Figure 10). While WTTS can be found over the entire region, the CTTS concentrate towards the regions of higher extinction and gas density delineating a ring-like structure

with a radius of $\sim 2^\circ$ (~ 15 pc at the 400 pc distance to OB1b). The center of the ring is located near the B0Iae star ϵ Ori, in a region of low A_V . This distribution is similar to that found in the molecular ring around λ Ori, which has comparable dimensions to the Ori OB1b ring ($\sim 16 - 20$ pc, Dolan & Mathieu 1999, 2001, 2002). Dolan & Mathieu (1999) found that only 5% of the stars near the center of the λ Ori ring are CTTS, while most CTTS concentrate near the molecular ring. These authors suggested that the lack of accreting stars near the center of the region could be the result of photoevaporation of disks by the nearby OB stars. Dolan & Mathieu proposed that the CTTS along the ring were formed by the effects of a supernova at the center of this structure, which snow-plowed pre-existing molecular material into dense enough concentrations to trigger star formation. On a smaller scale, a similar situation is also found by Sicilia-Aguilar et al. (2005) in a study of the young cluster Trumpler 37, where the CTTS are strongly concentrated in a region away from the central O star. Briceño et al. (2005) speculate that Ori OB 1b corresponds to a population formed by a supernova event which occurred near ϵ Ori ~ 5 Myr ago. Based on their findings, they redefined the boundaries of OB1b, so that it roughly follows the outer $A_V \sim 0.5$ contour at $\alpha_{J2000} \sim 82.5^\circ$ and is limited by the cloud at $\alpha_{J2000} \sim 85.5^\circ$.

In their recent search for Orion OB1 members in two fields surrounding the belt stars Mintaka (δ Ori) and Alnilam (ϵ Ori), Caballero & Solano (2008) report 47 confirmed stars around Mintaka, and 89 in the Alnilam field; for clarity, these sources are not plotted in Figure 10. Among the intermediate to low-mass stars, there are 18 in the Mintaka field and 40 in the Alnilam field. In the Mintaka field, 2 objects are CVSO stars from Briceño et al. (2005), one also in McGehee (2006), and 10 are Kiso $H\alpha$ emission stars without slit spectra. In the Alnilam field, 3 objects were reported by Alcalá et al. (1996), 7 by Béjar et al. (2003, only 3 have split spectra), 5 by Briceño et al. (2005). Among the remaining objects, 15 are $H\alpha$ emission sources from the Kiso objective prism surveys (Wiramihardja et al. 1989) and 1 from Stephenson (1986), all lacking slit spectra to confirm membership; there are 6 X-ray sources, four of which also have $H\alpha$ emission, though none have slit spectra. In the Herbig & Bell (1988) catalog only PU Ori is within the Alnilam field. Caballero & Solano (2008) investigated the spatial distribution of the likely members surrounding Alnilam and Mintaka. They find no compelling evidence for the reality of Collinder 70, also called the “ ϵ Ori cluster” (e.g. Béjar et al. 2003), at least not within their 45 arcmin search radius. Around δ Ori they find that the radial distribution of stars follows a power-law with an exponent 1-2. They argue that this odd value could be due to contamination from the foreground OB1a population; they call this concentration of likely PMS stars the “Mintaka cluster”, and propose it may be an evolved version of the σ Ori cluster.

The map of the dispersed PMS populations across Orion OB1 is allowing us to start building a 3-D picture of the giant molecular cloud out of which the Orion OB1 association formed. Once hundred of pcs in depth, it formed stars ~ 10 Myr ago in the side closer to Earth (the nearer OB1a association). While the gas in this part of the cloud has now dissipated, star formation is still actively proceeding on the far side, where molecular clouds A and B remain, containing a number of young and embedded clusters and many protostars (see chapters on L1630, L1641, OMC 2/3 in this volume). In between, a number of groups have been left behind, the footprint of star formation in this region (Figures 7,10). In Table 2 we summarize the properties of the Orion OB1 association as derived from the low-mass stars.

4.2. Young Brown Dwarfs and Very Low-mass PMS Stars

So far, only two studies have performed spectroscopic confirmation in searches for very low-mass PMS stars and young brown dwarfs in the off-cloud populations of the Orion OB1 association. In their survey near ϵ Ori, Béjar et al. (2003) identified 3 late type objects with $H\alpha$ in emission and Na I line strengths indicative of low gravity. With spectral types M4.5 to M6, equivalent to masses in the range $\sim 0.2 - 0.08 M_{\odot}$ (e.g. Baraffe et al. 1998), these are all very-low mass PMS stars and young objects at the substellar limit for this region.

Recently, in their large scale search for PMS objects down to below the substellar limit, Downes et al. (2006, 2008) identified one very low-mass star with spectral type M4.5, one object at the substellar limit, with spectral type M6, and one brown dwarf with a spectral type M7, in the Ori OB1a subassociation. They also found 19 new members in Ori OB1b, 14 very low-mass stars, out of which 7 have M6 spectral types, and 5 brown dwarfs (two with spectral types M6.5, two M7 and one M7.5). Summarizing, they confirmed 22 new members in the mass range $0.04 - 0.15 M_{\odot}$, 3 in Ori OB1a, one of which is substellar ($M \sim 0.07 M_{\odot}$), and 19 in Ori OB1b, out of which 7 are at the substellar limit and 5 are substellar ($M = 0.04 - 0.072 M_{\odot}$).

4.3. The 25 Orionis Cluster

Briceño et al. (2005) identified a clustering of low-mass, young stars around the early B-type star 25 Orionis (Figure 10). Through low-resolution follow up spectroscopy of CVSO candidates, Briceño et al. (2007b) confirmed nearly 200 PMS stars in this stellar aggregate.

They found that both the higher mass stars and the TTS in 25 Ori follow a relatively well defined band in the CMD (Figure 11). The spread observed is largely consistent with the upper limit of 0.75 magnitudes expected from unresolved binaries. By comparing with different isochrones they derive an age of 7-10 Myr. Parallaxes for the B and A-type stars in this group indicate that it is closer than the rest of Ori OB1. The 25 Ori cluster is the most populous ~ 10 Myr sample yet known within 500 pc.

Many clusters are known in the Orion molecular clouds (e.g. chapters by Peterson & Megeath, Allen & Davis, Muench et al., Walter et al. in this volume), but the high degree of spatial substructure among the off-cloud population, and the discovery of one cluster so far, has been a surprising new result from recent studies.

Briceño et al. (2007b) also conducted a radial velocity study of 147 TTS distributed in two 1 deg wide fields, one located on the 25 Ori group, and the other in the OB1b region, near the belt star ϵ Ori. They found that the 25 Ori members share a common velocity of 19.7 km s^{-1} , well differentiated from the $\sim 30 \text{ km s}^{-1}$ velocity that characterizes OB1b members (Figure 11), and also from the $\sim 24 \text{ km s}^{-1}$ velocity that Jeffries et al. (2006) assign to the widely distributed, general population of the OB1a sub-association. This confirmed that this aggregate is kinematically distinct from the background molecular cloud, and is probably a remnant of a now dissipated front end of the Orion giant molecular cloud.

As mentioned in Sect. 4., the presence of the Li I 6707 Å line strongly in absorption is a clear indicator of youth in K and M-type stars. Figure 12, shows the distribution of Li I equivalent widths, $W(\text{Li I})$, plotted as a function of the effective temperature for each star in the sample of Briceño et al. (2007b), compared with data for the ~ 2 Myr old Taurus region, the IC 2602 cluster (age ~ 30 Myr; Stauffer et al. 1997) and the Pleiades (age ~ 125 Myr; Stauffer et al. 1998). All the 25 Ori and

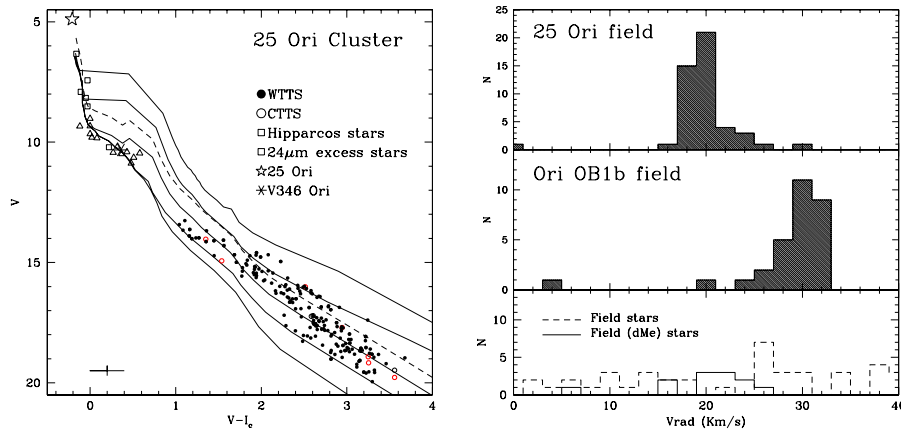


Figure 11. (adapted from Briceño et al. 2007b). Left: Color-magnitude diagram of PMS stars in the 25 Ori cluster. T Tauri stars are indicated with solid circles (WTTS) and open circles (CTTS). B type *Hipparcos* stars are shown as open squares. Open triangles are A-F stars with IR excesses at $24\ \mu\text{m}$ (Hernández et al. 2005). Isochrones (Siess et al. 2000) are shown as solid lines, from top to bottom: 1, 3, 10, 30 and 100 Myr (which we adopt as the ZAMS). The dashed line indicates the 0.75 magnitude offset for the 10 Myr isochrone, expected from unresolved binaries. The error bar at the lower left indicates the typical uncertainty of the photometry at the faint magnitude limit. Right: Histogram of heliocentric radial velocities of the 25 Ori cluster (upper panel) and a field in OB1b with radial velocities similar to those of the gas in the Orion molecular cloud (middle panel). The lower panel shows the distribution of radial velocities for field and dMe stars. Velocity bins are $2\ \text{km s}^{-1}$ wide. A clear difference of $\sim 10\ \text{km s}^{-1}$ exists between both regions, confirming the 25 Ori cluster as a distinct kinematic entity.

Ori OB1b members fall above the upper cluster envelopes; also, in both Orion regions the observed $W(\text{Li I})_{\text{max}} \sim 0.6$ is lower than in Taurus. Comparison of the $W(\text{Li I})$ shows that while 40% of all the Ori OB1b members fall within the Taurus TTS locus only 22% of the TTS in the 25 Ori group share this region of the diagram. The effects of Li depletion among the Orion populations, seen in the lower $W(\text{Li I})_{\text{max}}$ and the increasing fraction of TTS with $W(\text{Li I})$ values below the Taurus lower boundary as a function of age, are consistent with the ages derived for the Ori OB1b region and the 25 Ori aggregate, providing further support for a significant (by a factor $\sim 2x$) age difference between these two subassociations.

In his study, McGehee (2006) shows an excess of candidate PMS stars at $\alpha_{J2000} \sim 81^\circ$ and $\delta_{J2000} = +0.5^\circ$ to $+0.8^\circ$, which he identifies as the south tip of the 25 Ori cluster (Figure 8 of that article). Because of this he derives a cluster radius of 8-11 pc, and suggests that 25 Ori is an unbound association rather than an open cluster. However, it is not clear whether the feature identified by McGehee as the southern tip of the 25 Ori group is physically part of this stellar aggregate; radial velocities need to be obtained before these objects can be interpreted as belonging to the 25 Ori cluster. Briceño et al. (2007b) presented an initial investigation into the spatial structure of the 25 Ori group, and argued that the radius of the 25 Ori group is slightly smaller, ~ 7 pc, which combined with the seemingly large number of members brings into question the actual dynamical state of this stellar aggregate. Briceño et al. (2005) found a pronounced peak in the spatial distribution of low-mass young stars, with a density

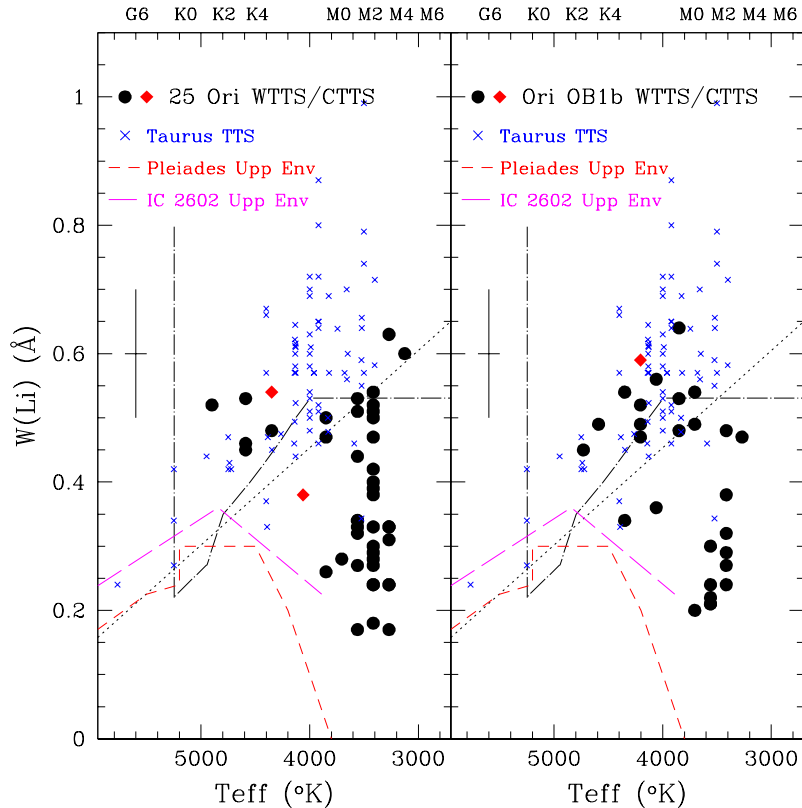


Figure 12. Equivalent width of the Li I 6707 Å line plotted against the effective temperature (from Briceño et al. 2007b). Left panel: stars in the 25 Ori cluster. Right panel: stars in the Orion OB1b region. WTTS are shown as dots and CTTS as diamonds. Taurus PMS stars (age $\sim 1 - 2$ Myr) are shown as \times 's (Basri et al. 1991; Martín et al. 1994). The dotted line traces the lower boundary to the majority of Taurus TTS. The long dash-dot line corresponds to the lithium isoabundance line from Martín (1997). The short-dash line is the upper envelope for the Pleiades cluster (age ~ 125 Myr; Stauffer et al. 1998; Soderblom et al. 1993; García-López et al. 1994), and in the long-dash line the upper envelope of the IC 2602 cluster (age ~ 30 Myr; Stauffer et al. 1997; Randich et al. 1997). The typical error bar is also indicated in each panel.

of 128 stars/deg², at $\alpha_{J2000} = 81.3^\circ$, $\delta_{J2000} = +1.5^\circ$, $23.6'$ south-east of 25 Ori (see Figure 7). The density of stars falls off significantly at a radius of $\sim 1.2^\circ$, which corresponds to 7 pc at the assumed distance of 330 pc. This value is slightly larger than what Sherry et al. (2004) found for the younger σ Ori cluster ($\sim 3 - 5$ pc). At a velocity dispersion of $\sim 1 \text{ km s}^{-1}$, an unbound stellar aggregate would expand roughly 1 pc every 1 Myr. If the 25 Ori group resembled the σ Ori cluster at an age of ~ 4 Myr, a naive dynamical picture would have it evolve to a cluster radius of $\sim 7 - 9$ pc at ~ 8 Myr. However, Briceño et al. (2007b) caution that because their member census of the 25 Ori region is not yet complete, especially north of $\delta_{J2000} = +2.13^\circ$, the actual membership and extent of the group may be larger.

Table 2. Orion OB1 properties derived from low-mass PMS stars

| Group | Age (Myr) | D (pc) | No. Stars ($M_* \lesssim 1M_\odot$) | CTTS fraction (%) |
|--------|--------------|-----------|--|----------------------|
| OB1a | 7-10 | 330 | 37 ¹ | 11 |
| OB1b | 4-6 | 440 | 142 | 12.6-23 |
| 25 Ori | 7-10 | 330 | 197 | 5.6 |

Ages and CTTS fractions are from Briceño et al. (2005, 2007b). Distances are from Brown et al. (1994).

¹: Number of widely spread PMS stars in OB1a so far, excluding the 25 Ori cluster.

5. The Initial Mass Function in the Orion Off-cloud Populations

The form of the Initial Mass Function (IMF) in OB associations is a crucial information to determine the number of low-mass stars formed in these regions, which was not well known until recently, as well as to gain insight into whether ambient conditions may affect the star formation process. If the IMF in OB associations is not truncated and similar to the field IMF, it would follow that most of their total stellar mass ($\gtrsim 60\%$) is found in low-mass ($< 2 M_\odot$) stars. This would then imply that most of the current Galactic star formation is taking place in OB associations (Briceño et al. 2007a).

Because low-mass PMS stars ($0.7 \gtrsim M/M_\odot \gtrsim 0.1$, equivalent to spectral types later than $\sim K7$) are mostly on their vertical Hayashi evolutionary tracks, spectral types roughly correspond to stellar mass, such that distributions of spectral types can be used as an approximate proxy of the IMF in these young regions (ages $\lesssim 10$ Myr; e.g. see Luhman et al. 2003b). Moreover, the spectral type is an easily observable quantity that can be well determined for M-type stars. Comparisons of these distributions among different regions have the advantage of providing a way to look for differences among IMFs without the mediation of theoretical evolutionary models, and the uncertainties and systematics involved in transforming observables such as magnitudes and spectral types to effective temperatures and luminosities.

Figure 13 shows the spectral type distributions from mid-K to late M of members of the 25 Ori cluster and the Orion OB1b region (data from Briceño et al. 2005, 2007b), and compare with similar histograms for the Orion Nebula Cluster (data from Hillenbrand 1997), the IC 348 cluster (data from Luhman et al. 2003b) and the Taurus star forming region (data from Luhman et al. 2006). These samples have all been derived using similar observational approaches, namely deep photometric searches followed by spectroscopic confirmation of members. Therefore, strong biases inherent to differing techniques like X-ray, objective prism surveys or proper motions, should be minimized.

The distributions for 25 Ori, Ori OB1b and the ONC look remarkably similar, all peaking at a spectral type M3. This would probably be expected if these populations do in fact share a common origin in the same giant molecular cloud complex (Briceño et al. 2007a). The histogram for IC 348 has a peak at a later spectral type of M5, and there seems to be a deficit of slightly higher mass TTS (spectral types earlier than $\sim M3$). The distribution of spectral types in Taurus is the one that seems to differ most respect to Orion; its peak is also located at M5, as in IC 348, but there is an excess of K7-M0

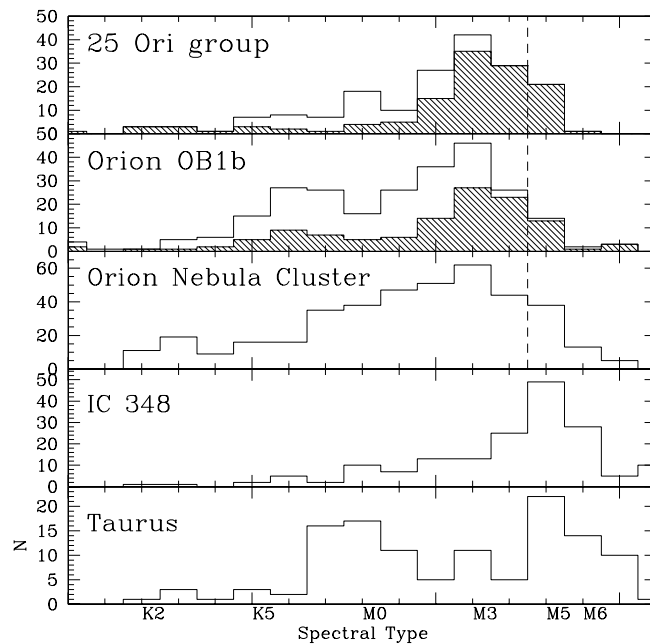


Figure 13. Distributions of spectral types for members of the 25 Ori group and the Orion OB1b subassociation (Briceño et al. 2005, 2007b), compared with the Orion Nebula Cluster (Hillenbrand 1997), IC 348 (Luhman et al. 2003b) and Taurus (Luhman et al. 2006). The filled histograms indicate the kinematic members in 25 Ori and OB1b. The vertical dashed lines in the Orion panels indicate the approximate completeness limit. For Taurus and IC 348 the completeness limit is beyond M7.

stars, or alternatively a deficit of M2-M4 objects. That the IMF in Taurus seems different to that in other regions has been noted by various authors (e.g. Briceño et al. 2002; Luhman et al. 2003a,b). The excess at K7-M0 was actually the peak of the distribution in earlier studies (e.g. Briceño et al. 2002; Luhman et al. 2003a; Luhman 2004b), which here is mitigated with the addition of a number of M5 and M6 new members by Luhman et al. (2006). However, Luhman et al. (2006) points out that there is an unknown level of incompleteness in the spectral type range M2-M6 because of a possible gap between the faint limits of the wide-field X-ray and objective prism surveys and the bright limits of deep optical broadband imaging surveys. The apparent shift in the peak of the distributions toward a later spectral type, between Orion and IC 348 and Taurus, could also be an incompleteness effect; being a factor of $3\times$ further away than Taurus and $1.5\times$ than IC 348, the magnitude limited searches in Orion have a larger low-mass limit (i.e., they are limited at an earlier spectral type).

Except for Taurus, the distributions in Figure 13 suggest a rough similarity between the IMF in these regions, at least within the spectral type range K3-M6. Luhman et al. (2003b) found that, at least down to spectral type \sim M6, the IC 348 IMF is consistent with that of the field, a result also obtained for the ONC by several authors (e.g. Hillenbrand 1997; also see chapter by Muench et al.). In the σ Ori cluster Sherry et al. (2004) found that the IMF in the range $0.1 - 1 M_{\odot}$ is consistent with the Kroupa (2002) field IMF (see chapter by Walter et al. in this volume). In the immediate vicinity of λ Ori,

Barrado y Navascués et al. (2004) derived an IMF from $0.02 - 1.2 M_{\odot}$ that is similar to that derived in other young regions like the ONC, α Per and the Pleiades. Over the entire λ Ori star-forming region, Dolan & Mathieu (2001) found that while the global IMF of the λ Ori SFR resembles the field, the IMF on smaller spatial scales appears to vary substantially (see chapter by Mathieu for a detailed discussion of the IMF in the λ Ori region). Summarizing, the variations in the details of the IMF among differing star-forming regions are still a matter of debate. As the census of low-mass stars in regions like the Orion OB1 association becomes more complete, we will be in a better position to assess whether real differences exist, that could be related to the initial conditions of the star formation process.

6. Circumstellar Disks and Accretion in Orion OB1a and OB1b

Circumstellar disks around young stars play an important role in determining the final mass of the star and as potential sites for planet formation. We now recognize that dust particles suspended in the disk gas evolve, with solids coagulating and settling toward the midplane (Weidenschilling 1997); this dust growth and settling are thought to be the first stage in planetary accumulation (Pollack et al. 1996).

The presence of disks can be inferred by optical signatures like strong emission in hydrogen Balmer lines like $H\alpha$, produced by hot ($T \sim 10^4$ K) gas flowing through a magnetosphere, and by excess IR emission from warm dust in the disk, heated by irradiation from the central star. In order to investigate how these disks evolve and may give rise to planetary systems, it is necessary to characterize their properties in young stellar populations, at ages up to ~ 10 Myr.

So far, the most extensive studies of how circumstellar disk fractions change with time have been conducted in the Orion OB1 association. However, the large majority of these investigations have concentrated on the youngest regions, or densest clusters (see Briceño et al. 2007a, for a review). Information on disks properties and fractions among the more widely spread PMS population has become available only very recently.

In the mass range $M \sim 0.3 - 1 M_{\odot}$, characteristic of low-mass PMS stars, several studies have started to search for disks among the dispersed TTS populations. Briceño et al. (2005), using the strong $H\alpha$ emission in CTTS as a proxy for disk accretion, and applying the CTTS/WTTS classification scheme by White & Basri (2003), derived the fraction of accreting CTTS across Ori OB1. They obtained an accretor fraction of 11% in Ori OB1a and 23% in OB1b. They compared their estimates with other regions in their Figure 12. Briceño et al. (2007b), also counting the number of CTTS, found an accretor fraction of 5.6% in the 25 Ori cluster, while in a Ori OB1b field, next to the belt star ϵ Ori, the CTTS fraction is 12.6%. These values are almost a factor of ~ 2 lower than those reported in Briceño et al. (2005). However, they argued that the apparent discrepancy can be explained because the Ori OB1b sample in Briceño et al. (2005) included very young regions like the area in and around the NGC 2024 cluster ($\lesssim 1$ Myr) which has a large number of CTTS, and is nominally located within the Warren & Hesser (1977) Ori OB1b boundaries. Second, as the census of PMS stars in older regions like Ori OB1a increases, the most frequent type of members are WTTS, which tends to lower the accretor fraction.

McGehee (2006) combined the SDSS g , r , i , and z bands with 2MASS JHK magnitudes, to construct reddening-invariant indices and classify WTTS and CTTS candidates (see Sect. 3.4.). He found a CTTS fraction of $\sim 10\%$, similar to what

Briceño et al. (2005, 2007b) derived. Despite what the absolute CTTS fractions may be in each region, what does seem like a robust result is the decline of a factor $\sim 2\times$ in the number of accreting stars between the ~ 4 Myr old OB1b and the 7-10 Myr old OB1a.

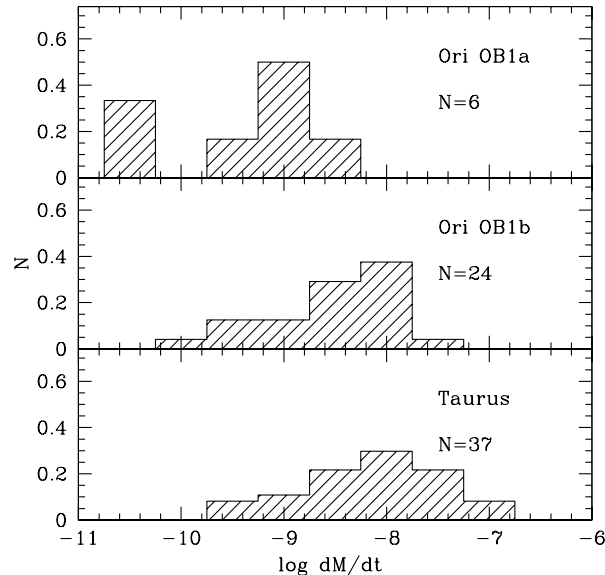


Figure 14. Distribution of the disk mass accretion rates for Ori1 OB1a (upper panel), Ori OB1b (middle panel) and Taurus (lower panel), from Calvet et al. (2005a).

Calvet et al. (2005a) combined UV, optical, JHKL and $10\ \mu\text{m}$ measurements in a sample of confirmed members of the OB1a and OB1b sub-associations to study dust emission and disk accretion. They showed evidence for an overall decrease in IR emission with age, interpreted as a sign of dust evolution between disks in Ori OB1b (~ 4 Myr), Ori OB1a (~ 8 Myr), and those of younger populations like Taurus (~ 2 Myr).

Figure 14 shows the distribution of the mass accretion rates derived by Calvet et al. (2005a) in Ori OB1a and OB1b, compared with determinations for the Taurus star-forming region (mass accretion rates in Taurus are from Gullbring et al. 1998; Hartmann et al. 1998). The age of the three populations increases from bottom to top. In all three cases, there is a large spread in the values of \dot{M} . However, as time proceeds, the number of rapid accretors decreases, and only low accretors remain in OB1a. Calvet et al. (2005a) applied statistical tests and concluded that the distributions of accretion rates are significantly different between the three regions. This decrease of \dot{M} with age qualitatively agrees with expectations from viscous disk evolution. However, viscous evolution alone cannot explain the decreasing fraction of accreting objects with age (Muzerolle et al. 2000; Briceño et al. 2005, 2007b); other factors (e.g. inner disk clearing associated with planet formation, Calvet et al. 2002; D’Alessio et al. 2005) must also play a role in slowing accretion onto the central star.

More recently, Hernández et al. (2007b) used IRAC and MIPS on Spitzer to look for dusty disks in Ori OB1a and OB1b (left panel of Figure 15). They found a number of “transition” disk systems, objects with essentially photospheric fluxes at wavelengths $\leq 4.5\ \mu\text{m}$ and excess emission at longer wavelengths. These objects can be seen in the

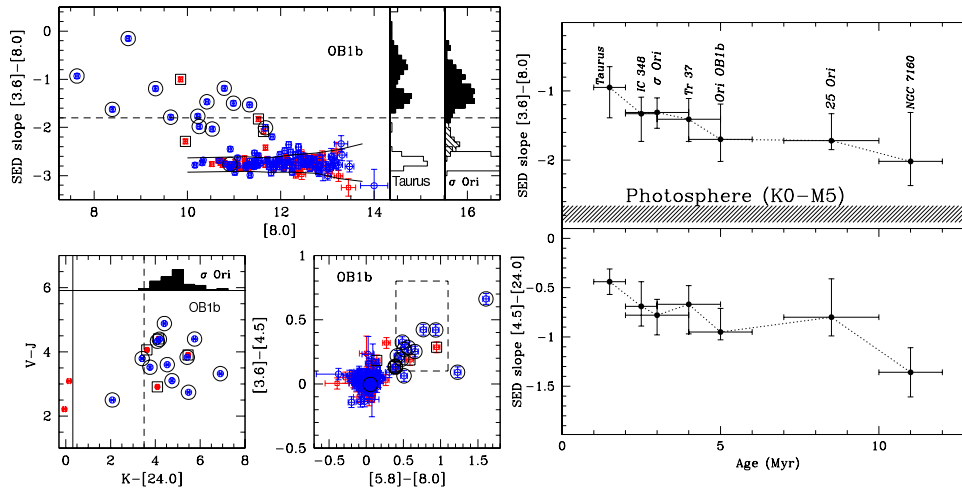


Figure 15. Left: Detecting disks with Spitzer (from Hernández et al. 2007b). Members are shown as circles, photometric candidates as squares, large symbols represent stars with excess at $24 \mu\text{m}$. Solid histograms indicate IRAC spectral energy distribution slopes for stars with optically thick disks in Taurus (Hartmann et al. 2005) and the σ Ori cluster (Hernández et al. 2007a); open histograms are stars with no IRAC excesses. The hatched histogram are objects with evolved disks in σ Ori (Hernández et al. 2007a). Top: IRAC spectral energy slopes indicating stars with excess at $8 \mu\text{m}$. The photospheric locus is indicated by the solid lines. Objects located above the horizontal dashed line are considered to contain optically thick disks. Bottom-left: CVSO-2MASS-MIPS color-color diagram indicating stars with excess emission at $24 \mu\text{m}$. The vertical solid line indicates the photospheric level, and the dashed line represents the optically thick disk region limit (Hernández et al. 2007a). Bottom-right: IRAC color-color diagram. The locus of accreting stars is indicated with a dashed line box (D’Alessio et al. 2005). Right: Disk evolution. Upper right: median slope of the spectral energy distributions between $3.6 \mu\text{m}$ and $8 \mu\text{m}$ for various stellar groups, including 25 Ori and σ Ori. ”Error bars” are quartiles, i.e., 50% of the observations are within these bars. Lower right: similar plot for the IRAC $3.6 \mu\text{m}$ and MIPS $24 \mu\text{m}$ bands.

left plot of Figure 15 (top and lower left panels) as those symbols falling between the photospheric locus and the horizontal (or vertical) dashed line that limits the region were optically thick disks are located. These systems are interpreted as showing signatures of inner disk clearing, with optically thin inner regions stretching out to one or a few AU (Calvet et al. 2002; Uchida et al. 2004; Calvet et al. 2005b; D’Alessio et al. 2005; Espaillat et al. 2007). They found one transition disk system in 25 Ori and 3 in OB1b, which represents $\sim 10\%$ of the disk-bearing stars, indicating that the transitional disk phase is short, and therefore hinting at a rapid shut off of the accretion phase in these systems.

Hernández et al. (2007b) derived disk fractions of 6% in the 25 Ori aggregate and 13% in Ori OB1b, similar to what Briceño et al. (2007b) found from accretion indicators. Hernández et al. (2007b) also confirmed a decline in IR emission by the age of Orion OB1b and, by comparing the infrared excess in the IRAC and MIPS bands among several stellar groups, show that not only does inner disk emission decay with stellar age, but the inner disk dissipates more rapidly. In the upper right panel of Figure

15 there is a clear decrease of the median slope of the IRAC spectral energy distribution with age, approaching the photospheric limit, indicating a decrease of optical depth as dust grows and settles. There is also a decrease in the slope of the spectral energy distribution in the IRAC-MIPS diagram (lower right panel in Figure 15), but slower than in the IRAC-only plot; the IRAC-MIPS slope corresponds to regions further out in the disk than the IRAC-only slope. The faster decrease in the IR dust emission from the inner parts of the disk is indicative of an “inside-out” clearing.

In their sample of very low-mass TTS and young brown dwarfs, Downes et al. (2008) looked for the presence of accretion signatures by measuring the strength of the $H\alpha$ line in emission. Using the criteria by White & Basri (2003) they classified their new members as having CTTS or WTTS nature. They found that the 3 new members confirmed in Ori OB1a are WTTSs, while $39^{+25}_{-22}\%$ of the new members in Ori OB1b exhibit CTTS-like behavior, suggestive of ongoing accretion from a circum(sub)stellar disk. They also found that none of the members confirmed in OB1a show near-IR color excess while $38^{+26}_{-21}\%$ of OB1b members show H-K color excess. These results are consistent with findings by Briceño et al. (2005) for higher mass TTS in Orion OB1. The similarity in CTTS-like properties and near-IR excess across the substellar boundary gives support to the idea of a common formation mechanism for low mass stars and at least the most massive brown dwarfs.

Finally, among the higher mass members of the widely spread PMS population of Ori OB1 and OB1b (stars of spectral types B, A and F), so far only two studies have looked for circumstellar disks. Hernández et al. (2005) carried out a study of the early-type stars in Orion OB1 (among other nearby OB associations), in order to identify Herbig Ae/Be (HAeBe) type stars, the PMS higher mass counterpart of TTS. They studied B, A, and F stars with membership determined from Hipparcos data. Comparing the data from associations with different ages, and assuming that the near-IR excess in the HAeBe stars arises from optically thick dusty inner disks, they found that the inner disk frequency in the age range 3-10 Myr in these higher mass stars is lower than that in the low-mass stars ($< 1 M_{\odot}$), in particular, a factor of ~ 10 lower at ~ 3 Myr. This indicates that the timescale for disk evolution is much shorter in young stars with masses in the range $2 M_{\odot} \lesssim M \lesssim 10 M_{\odot}$, which could be a consequence of more efficient mechanisms of inner disk dispersal.

Hernández et al. (2006) compared Spitzer $24 \mu\text{m}$ observations of B, A and F stars in Ori OB1a and OB1b with similar objects in other stellar groups, spanning a range of ages from 2.5 to 150 Myr, and found that debris disks are more frequent and have larger $24 \mu\text{m}$ excess at ages ~ 10 Myr (OB1a). This trend agrees with predictions of models of evolution of solids in the outer regions of disks (> 30 AU; e.g. Kenyon & Bromley 2005), where large icy objects (~ 1000 km) begin to form at ~ 10 Myr; the presence of these objects in the disk initiates a collisional cascade, producing enough dust particles to explain the relatively large $24 \mu\text{m}$ excesses observed in Ori OB1a. Combining Spitzer observations, optical spectra, and 2MASS data, they also identified a new Herbig Ae/Be star (HD 290543) and a star (HD 36444) with a large $24 \mu\text{m}$ excess, both in OB1b. This last object can be explained as an intermediate stage between a Herbig Ae/Be type object (which harbor optically thick disks) and true debris systems, or alternatively as a massive debris disk produced by a collision between two large objects (> 1000 km).

Acknowledgements. I am deeply indebted to my close collaborators Nuria Calvet, Lee Hartmann, Jesus Hernández, Kathy Vivas, Juan Jose Downes, Lori Allen and James

Muzerolle; without their hard work, deep insight and lively discussions the PMS map of the Orion OB1 association would still be largely blank; all the merits of the CIDA Variability Survey of Orion (CVSO) and related studies are theirs, the errors are solely mine.

The CVSO has been made possible by the continuous efforts of the CIDA staff, observers and Night Assistants, in particular, O. Contreras, F. Moreno, G. Rojas and U. Sanchez, technical staff, especially Gerardo Sánchez, and through the painstaking work by Perry Berlind and Mike Calkins at SAO, who have obtained spectra for thousands of candidate PMS stars in Orion. I also thank Susan Tokarz at CfA for the reduction of the spectroscopic material obtained at SAO. I am grateful to the referee for useful comments, and very specially to the editor, Bo Reipurth, for his endless patience and his further input to the manuscript. The CVSO has received support from grants S1-2001001144 of FONACIT, Venezuela, NSF grant AST-9987367 and NASA grant NAG5-10545.

Much of the results compiled here are based on observations obtained at the Llano del Hato National Astronomical Observatory of Venezuela, operated by CIDA for the Ministerio de Ciencia y Tecnología, and at the Fred Lawrence Whipple Observatory of the Smithsonian Institution, USA.

References

- Alcalá, J. M., Terranegra, L., Wichmann, R., Chavarría-K., C., Krautter, et al. 1996, *A&AS*, 119, 7
- Baade, W. & Minkowski, R. 1937, *ApJ*, 86, 119
- Bally, J., Stark, A. A., Wilson, R. W., & Langer, W. D. 1987, *ApJ*, 312, L45
- Baltay, C., Snyder, J.A., Andrews, P. et al. 2002, *PASP*, 114, 780
- Baraffe, I., Chabrier, G., Allard, F., & Hauschildt, P.H. 1998, *A&A*, 337, 403
- Barrado y Navascués, D., Béjar, V. J. S., Mundt, R., Martín, E. L., Rebolo, R., et al. 2003, *A&A*, 404, 171
- Barrado y Navascués, D., & Martín, E. L. 2003, *AJ*, 126, 2997
- Barrado y Navascués D., Stauffer J. R., Bouvier J., Jayawardhana R., & Cuillandre J-C. 2004, *ApJ*, 610, 1064
- Basri, G., Martín, E. L., & Bertout, C. 1991, *A&A*, 252, 625
- Béjar, V. J. S., Zapatero Osorio, M. R., & Rebolo, R. 1999, *ApJ*, 521, 671
- Béjar, V. J. S., Rebolo, R., Zapatero Osorio, M. R., & Caballero, J. A. 2003, in *The Future of Cool-Star Astrophysics: 12th Cambridge Workshop on Cool Stars, Stellar Systems, and the Sun*, eds. A. Brown, G.M. Harper, & T.R. Ayres, (University of Colorado), 651
- Blaauw, A. 1964, *ARA&A*, 2, 213
- Blaauw, A. 1991, in *The Physics of Star Formation and Early Stellar Evolution*, eds. C. Lada and N.D. Kylafis, (Dordrecht: Kluwer), p. 125
- Briceño, C., Hartmann, L., Stauffer, J., Gagne, M., Caillault, J.-P., & Stern, A. 1997, *AJ*, 113, 740.
- Briceño C., Hartmann L., Calvet N., & Kenyon, S. 1999, *AJ*, 118, 1354
- Briceño C., Vivas A. K., Calvet N., Hartmann L., Pacheco, R., et al. 2001, *Sci*, 291, 93
- Briceño, C., Luhman, K. L., Hartmann, L., Stauffer, J. R., & Kirkpatrick, J. D. 2002, *ApJ*, 580, 317
- Briceño C., Calvet N., Hernández J., Vivas A. K., Hartmann L., et al. 2005, *AJ*, 129, 907
- Briceño, C., Preibisch, T., Sherry, W. H., Mamajek, E. E., Mathieu, R. D., Walter, F. M., & Zinnecker, H. 2007a, in *Protostars & Planets V*, eds. B. Reipurth, D. Jewitt, & K. Keil, (Tucson: University of Arizona Press), p. 345
- Briceño C., Hartmann, L., Hernández J., Calvet, N., Vivas A. K., et al. 2007b, *ApJ*, 661, 1119
- Briceño, C. et al. 2008, *AJ*, in preparation

- Brown, A. G. A., de Geus, E. J., & de Zeeuw, P. T. 1994, *A&A*, 289, 101
- Brown, A. G., Walter, F. M., & Blaauw, A. 1999, in *ASP Conf. Ser., The Orion Complex Revisited*, ed. M.J. McCaughrean & A. Burkert, unpublished
- Caballero, J. A. & Solano, E. 2008, *A&A*, 485, 931
- Calvet N., D'Alessio P., Hartmann L., Wilner D., Walsh A., & Sitko M. 2002, *ApJ*, 568, 1008
- Calvet N., Briceño C., Hernández J., Hoyer S., Hartmann L., et al. 2005a, *AJ*, 129, 935
- Calvet N., D'Alessio P., Watson D. M., Franco-Hernández R., Furlan E. et al. 2005b, *ApJ*, 630, L185
- Cameron, F., Rieke, G. H., & Rieke, M. J. 1996, *ApJ*, 473, 294
- Crawford, D. L. & Barnes, J. V. 1966, *AJ*, 71, 610
- Dahari, D. B. & Lada, E. A. 1999, American Astronomical Society, 195th AAS Meeting, #79.13; *Bulletin of the American Astronomical Society*, 31, 1491
- D'Alessio P., Hartmann L., Calvet N., Franco-Hernández R., Forrest W. et al. 2005, *ApJ*, 621, 461
- Dolan, C. J. & Mathieu, R., D. 1999, *AJ*, 118, 2409
- 2001, *AJ*, 121, 2124
- 2002, *AJ*, 123, 387
- Downes, R. A. & Keyes, C. D. 1988, *AJ*, 96, 777
- Downes, J. J., Briceño, C., & Hernández, J. 2006, *Revista Mexicana de Astronomía y Astrofísica, Conference Series*, 26, 37
- Downes, J. J., Briceño, C., Hernández, J., Calvet, N., Hartmann, L., & Ponsot Balaguer, E. A. 2008, *AJ*, 136, 51
- Españolat, C., Calvet, N., D'Alessio, P., Hernández, J., Qi, C., et al. 2007, *ApJ*, 670, L135
- Feigelson E. D. & DeCampli W. M. 1981, *ApJ*, 243, L89
- Feigelson E.D., Broos P., Gaffney III J.A., Garmire G., Hillenbrand L.A., et al. 2002, *ApJ*, 574, 258
- Feigelson, E. D., Gaffney, J. A., III, Garmire, G., Hillenbrand, L. A., & Townsley, L. 2003, *ApJ*, 584, 911
- Freyberg, M. J. & Schmitt, J. H. M. M. 1995, *A&A*, 296, 21
- Gagné M. & Caillault J.-P. 1994, *ApJ*, 437, 361
- García-López, R. J., Rebolo, R., & Martín, E. L. 1994, *A&A*, 282, 518
- Gaustad, J. E., McCullough, P. R., Rosing, W., & Van Buren, D. 2001, *PASP*, 113, 1326
- Genzel, R., Reid, M. J., Moran, J.M., & Downes, D. 1981, *ApJ*, 244, 884
- Genzel, R. & Stutzki, J. 1989, *ARA&A*, 27, 41
- Getman K.V., Feigelson E.D., Grosso N., McCaughrean M.J., Micela G., et al. 2005, *ApJS*, 160, 353
- Gómez, M. & Lada, C. J. 1998, *AJ*, 115, 1524
- Gullbring, E., Hartmann, L., Briceño, C., & Calvet, N., 1998, *ApJ*, 492, 323
- Gutermuth, R. A., Pipher, J. L., Myers, P. C., Megeath, T. S., Allen, L. E., & Allen, T. 2006, *AAS*, 208, No.8.07
- Haisch, K. E., Jr., Lada, E. A., & Lada, C. J. 2000, *AJ*, 120, 1396
- Haisch, K. E., Jr., Lada, E. A., Piña, R. K., Telesco, C. M., & Lada, C. J. 2001, *AJ*, 121, 1512
- Hardie, R. H., Heiser, A. M., & Tolbert, C. R. 1964, *ApJ*, 140, 1472
- Hartmann, L., Calvet, N., Gullbring, E. & D'Alessio, P. 1998, *AJ*, 495, 385
- Hartmann, L., Calvet, N., Watson, D.M. et al. 2005, *ApJ*, 628, L147
- Harvey, P. M., Campbell, M. F., Hoffmann, W. F., Thronson, H. A., Jr., & Gatley, I. 1979, *ApJ*, 229, 990
- Herbig, G.H. 1962, *Adv. Astron. Astrophys.* 1, 47
- Herbig, G. H. & Terndrup, D.M. 1986, *ApJ*, 307, 609
- Herbig G. H. & Bell K. R. 1988, *Lick Observatory Bulletin No. 1111*, Lick Observ., Santa Cruz
- Herbig, G. H. & Kuhl, L. V. 1963, *ApJ*, 137, 398
- Herbig, G. H. & Rao, N. K. 1972, *ApJ*, 174, 401
- Herbst, W., Rhode, K. L., Hillenbrand, L. A., & Curran, G. 2000, *AJ*, 119, 261
- Hernández J., Calvet, N., Hartmann, L., Briceño, C., Sicilia-Aguilar, A., & Berlind, P. 2005, *AJ*, 129, 856

- Hernández, J., Briceño, C., Calvet, N., Hartmann, L., Muzerolle, J., & Quintero, A. 2006, ApJ, 652, 472
- Hernández, J., Hartmann, L., Megeath, T., Gutermuth, R., Muzerolle, J. et al. 2007a, ApJ, 662, 1067
- Hernández, J., Calvet, N., Briceño, C., Hartmann, L., Vivas, A. K., et al. 2007b, ApJ, 671, 1784
- Hillenbrand L. A. 1997, AJ, 113, 1733
- Hillenbrand, L. A., Strom, S. E., Calvet, N., Merrill, K. M., Gatley, I. et al. 1998, AJ, 116, 1816
- Jeffries, R. D., Maxted, P. F. L., Oliveira, J. M., & Naylor, T. 2006, MNRAS, 371, 6
- Johnson, H. M. 1965, ApJ, 142, 964
- Joy A. H. 1945, ApJ, 102, 168
- Kenyon, S. J. & Bromley, B. C. 2005, AJ, 130, 269
- Kenyon, S. J. & Hartmann, L., 1995, ApJS, 101, 117
- Kenyon, M. J., Jeffries, R. D., Naylor, T., Oliveira, J. M., & Maxted, P. F. L. 2005, MNRAS, 356, 89
- Kirkpatrick, J. D., Reid, I. N., Liebert, J., Cutri, R. M., Nelson, B. et al. 1999, ApJ, 519, 802
- Kogure, T., Yoshida, S., Wiramihardja, S., Nakano, M., Iwata, T. & Ogura, K. 1989, PASJ, 41, 1195
- Kroupa P. 2002, Sci, 295, 82
- Kutner, M. L., Tucker, K. D., Chin, G., & Thaddeus, P. 1977, ApJ, 215, 521
- Lada C. J. & Lada, E. A. 2003, ARA&A, 41, 57
- Lamm, M. H., Bailer-Jones, C. A. L., Mundt, R., Herbst, W., & Scholz, A. 2004, A&A, 417, 557
- Levine, J. L., Steinhauer, A., Elston, R. J., & Lada, E. A. 2006, ApJ, 646, 1215
- Luhman, K. L., Briceño, C., Stauffer, J. R., Hartmann, L., Barrado y Navascués, D., & Caldwell, N. 2003a, ApJ, 590, 348
- Luhman, K. L., Stauffer, J. R., Muench, A. A., Rieke, G. H., Lada, E. A., et al. 2003b, ApJ, 593, 1093
- Luhman, K. L. 2004a, ApJ, 602, 816
- Luhman, K. L. 2004b, ApJ, 617, 1216
- Luhman, K. L., Whitney, B. A., Meade, M. R., Babler, B. L., Indebetouw, R., Bracker, S., & Churchwell, E. B. 2006, ApJ, 647, 1180
- Lynds, B. T. 1962, ApJS, 7, 1
- Maddalena, R. J., Morris, M., Moscovitz, J., & Thaddeus, P. 1986, ApJ, 303, 375
- Maheswar, G., Manoj, P. & Bhatt, H. C. 2003, A&A, 402, 963
- Martín, E. L., Rebolo, R., Magazzu, A., & Pavlenko, Ya. V. 1994, A&A, 282, 503
- Martín, E. L. 1997, A&A, 321, 492
- McGehee P. M., West A. A., Smith J. A., Anderson, K. S. J., & Brinkmann J. 2005, AJ, 130, 1752
- McGehee, P. M. 2006, AJ, 131, 2959
- Muzerolle, J., Calvet, N., Briceño, C., Hartmann, L., & Hillenbrand, L. 2000, ApJ, 535, L47
- Muzerolle, J., Young, E., Megeath, S. T., & Allen, L. 2005, in *Star Formation in the Era of Three Great Observatories*, meeting abstracts from the conference held July 13-15, 2005 in Cambridge, MA. <http://cxc.harvard.edu/stars05/agenda/program.html>, p. 41.
- Pollack, J. B., Hubickyj, O., Bodenheimer, P., Lissauer, J. J., Podolak, M., & Greenzweig, Y. 1996, Icarus, 124, 62
- Preibisch, T., McCaughrean, M. J., Grosso, N., Feigelson, E. D., Flaccomio, E., et al. 2005, ApJS, 160, 582
- Ramírez S. V., Rebull L., Stauffer J., Strom S., Hillenbrand L., et al. 2004, ApJ, 128, 787
- Randich, S., Aharpour, N., Pallavicini, R., Prosser, C. F., & Stauffer, J. R. 1997, A&A, 323, 86
- Rebull, L. M., Hillenbrand, L. A., Strom, S. E., Duncan, D. K., Patten, B. M., et al. 2000, ApJ, 119, 3026
- Sanduleak N. 1971, PASP, 83, 95
- Schlegel, D.J., Finkbeiner, D.P., & Davis, M. 1998, ApJ, 500, 525
- Scholz, A. & Eisloffel, J. 2005, A&A, 429, 1007
- Sherry W. H. 2003, PhD Thesis, SUNY, Stony Brook

- Sherry, W. H., Walter, F. M., & Wolk, S. J. 2004, AJ, 128, 2316
- Sicilia-Aguilar, A., Hartmann, L. W., Szentgyorgyi, A. H., Fabricant, D. G., Furész, G., et al. 2005, AJ, 129, 363
- Siess, L., Dufour, E., & Forestini, M. 2000, A&A, 358, 593
- Skinner, S. Gagné, M., & Belzer, E. 2003, ApJ, 598, 375
- Slesnick, C. L., Carpenter, J. M., & Hillenbrand, L. A. 2006, AJ, 131, 3016
- Soderblom, D. R., Jones, B. F., Balachandran, S., Stauffer, J. R., Duncan, D. K., et al. 1993, AJ, 106, 1059
- Stassun, K. G., van den Berg, M., Feigelson, E., & Flaccomio, E. 2006, ApJ, 649, 914
- Stauffer, J. R., Hartmann, L. W., Prosser, C. F., Randich, S., Balachandran, S., et al., 1997, ApJ, 479, 776
- Stauffer, J. R., Schultz, G., & Kirkpatrick, J. D. 1998, ApJ, 499, 199
- Stephenson, C. B. 1986, ApJ, 300, 779.
- Sterzik, M. F., Alcalá, J. M., Neuhäuser, R., & Schmitt, J. H. M. M. 1995, A&A, 297, 418
- Tsujimoto M. , Koyama K., Tsuboi Y., Goto M., & Kobayashi N. 2002, ApJ, 566, 974
- Uchida K. I., Calvet N., Hartmann L., Kemper F., Forrest W. J., et al. 2004, ApJS, 154, 439
- Voges W. , Aschenbach B., Boller T., Braeuninger H., Briel U., et al. 1999, A&A, 349, 389
- Walker, M. F. 1969 ApJ, 155, 447
- Walter F. M. & Kuhi L. V. 1981, ApJ, 250, 254
- Walter F. M. & Myers P. C. 1986, in *IV Cambridge Workshop on Cool Stars, Stellar Systems, and the Sun*, M. Zeilik & D. M. Gibson (eds.), 254, p. 55. Springer-Verlag, Berlin-Heidelberg-New York.
- Walter, F. M., Wolk, S. J., Freyberg, M., & Schmitt, J. H. M. M. 1997, *Memorie della Societa Astronomia Italiana*, 68, 1081
- Warren, W.H. & Hesser, J.E. 1977, ApJS, 34, 115
- Warren, W.H. & Hesser, J.E. 1978, ApJS, 36, 497
- Weaver W. B. & Babcock A. 2004, PASP, 116, 1035
- Weidenschilling, S. J. 1997, *Lunar and Planetary Institute Conference Abstracts*, 28, 1517
- White, R.J. & Basri, G. 2003, ApJ, 582, 1109
- Wiramihardja, S., Kogure, T., Yoshida, S., Ogura, K., & Nakano, M. 1989, in *IAUS No. 135 Interstellar Dust*, NASA N91-14897 06-88, p. 239
- Wiramihardja, S., Kogure, T., Yoshida, S., Nakano, M., Ogura, K., & Iwata, T. 1991, PASJ, 43, 27
- Wiramihardja, S., Kogure, T., Yoshida, S., Ogura, K., & Nakano, M. 1993, PASJ, 45, 643
- Wolk, S. J., Harnden, F. R., Jr., Flaccomio, E., Micela, G., Favata, F., et al. 2005, ApJS, 160, 423
- Yamauchi S. , Koyama K., Sakano M., & Okada K. 1996, PASJ, 48, 719
- Zapatero Osorio, M. R., Béjar, V. J. S., Pavlenko, Ya., Rebolo, R., Allende Prieto, C., et al. 2002, A&A, 384, 937